UNIVERSITY OF
CALIFORNIA

Radiation
Laboratory

GAMMA TRANSITIONS FROM THE 15-Mev LEVEL IN CARBON-12

BERKELEY, CALIFORNIA

DISCLAIMER

UCRL-3901
Physics and Mathematics

UNIVERSITY OF CALIFORNIA
Radiation Laboratory
Berkeley, California

Contract No. W-7405-eng-48

GAMMA TRANSITIONS FROM THE 15-Mev LEVEL IN CARBON-12

Charles N. Waddell

(Thesis)

August 13, 1957

Printed for the U.S. Atomic Energy Commission

GAMMA TRANSITIONS FROM THE 15-Mev LEVEL IN CARBON-12

Contents

GAMMA TRANSITIONS FROM THE 15-Mev LEVEL IN CARBON-12

Charles N. Waddell

Radiation Laboratory
University of California
Berkeley, California

August 13, 1957

ABSTRACT

The radiative transitions from the 15.1-Mev T = 1 level of C^{12} have been observed with a pair spectrometer and a NaI(Tl) crystal. The spectrum measured at 80^{o} with respect to the direction of a 31-Mev proton beam incident on a thick carbon target shows gamma rays of 15.1, 12.8, and 10.7 Mev with relative intensities of 1: 0.090 ± 0.015 : 0.095 ± 0.014. The 10.7-Mev gamma ray results from the transition to the first excited state of C^{12} and the 12.8± 0.2-Mev gamma ray can be identified as the ground-state transition from the 12.76-Mev level of C^{12}.

The excitation function for the production of the 15.1-Mev level by the inelastic scattering of protons has been measured from threshold to 340 Mev. The variation in yield near threshold is consistent with that expected from penetration of the Coulomb barrier by l = 0 outgoing protons. The variation in yield for higher-energy protons ($\sim$60 to 340 Mev) is in agreement with calculations based on the assumption of excitation through the collision of the incoming proton with a nucleon within the entire volume of a spherical nucleus.

The relative intensity of 15.1-Mev and 4.43-Mev gamma rays obtained in reactions inhibited by the conservation of isotopic spin has been compared with the relative intensity obtained in allowed reactions. In each of the allowed reactions—$C^{12}(p,p')C^{12*}$, $C^{12}(n,n')C^{12*}$, $B^{11}(d,n)C^{12*}$, $Be^{9}(\alpha,n)C^{12*}$—there was an observable yield of 15.1-Mev gamma rays. In the forbidden reactions—$C^{12}(d,d')C^{12*}$, $C^{12}(\alpha,\alpha')C^{12*}$—there was no observable yield until the energies of the incoming particles were sufficiently high to permit breakup of the outgoing particles. The measurements indicate that mixing of isotopic spins in the first T = 1 level is comparable to the mixing expected for the ground state.

Introduction

In connection with studies of proton bremsstrahlung,[1,2] in which a 180° pair spectrometer was used to analyze the photon spectrum, a gamma ray of 15.2 ± 0.2 Mev was observed superimposed on the bremsstrahlung spectrum when carbon was used as a target.[3] Upon consulting the literature[4] we could find no evidence for the emission of a gamma ray of this energy from any of the light nuclei, although there was evidence for a 15.09-Mev level in the neutron spectrum from $B^{11}(d,n)C^{12*}$.[5] All nuclei except He^4 are unstable against particle emission when excited to 15 Mev. However, for the Be^8 and C^{12} nuclei, alpha emission is the only mode of particle decay available at 15 Mev excitation energy. Since the alpha particle has no spin, the selection rules arising out of the need to conserve parity and angular momentum can prohibit α emission from an excited state, leaving γ emission as the only available mode of decay.

A well-known example of this phenomenon is found in the formation of the 17.63-Mev excited state of Be^8 by the resonant capture of 440-kev protons by Li^7.[6] It has been established that this state has J = 1 and even parity, and hence cannot decay into two α particles.[4,7] This state decays through the emission of a 17.6-Mev γ ray to the ground state, and of a 14.4-Mev γ ray to the first excited state of Be^8.

The question then arises, is there a similar situation existing to prohibit the emission of an α particle from a 15-Mev state in C^{12} ? The 0^+ ground state and the 2^+ first excited state of Be^8 are accessible to α decay with an energy release of 7.7 and 4.8 Mev respectively. Knowledge of the spins and parities of the final states would permit the assignment of the spin and parity of the excited state in C^{12} upon determinination of the orbital angular momentum involved in such a decay. Examination of Table I indicates that the laws of conservation of angular momentum and parity do not prohibit α emission from a 15-Mev state of spin and parity that permit an electromagnetic transition to the ground state.

Table I

Conservation of angular momentum and of parity in alpha decay of an excited state of C^{12}

If the Be^8 final state is	and the orbital angular momentum is	then the initial state in C^{12} is
0^+	$\ell = 0$ (s)	0^+
	$\ell = 1$ (p)	1^-
	$\ell = 2$ (d)	2^+
2^+	$\ell = 0$ (s)	2^+
	$\ell = 1$ (p)	1^- or 3^-
	$\ell = 2$ (d)	$1^+, 2^+, 3^+$ or 4^+

This fact suggested the very unpleasant possibility that there could conceivably have been error in the calibration of the pair spectrometer by the floating-wire technique, and that we were indeed (as suggested by others) seeing the γ rays from the 17.6-Mev level of Be^8. Accordingly the 20-ton pair-spectrometer magnet was moved to the rear of the Linear Accelerator Building so that we could look at the γ rays from Be^{8*}. The Van de Graaff injector was used to accelerate protons, which were captured in a thick Li^7 target and produced Be^{8*}. This experiment verified the calibration technique and clearly established that we were not seeing the decay of the 17.6-Mev state of Be^8.

We therefore had the task of determining whether the γ ray came from a state in Be^8 or C^{12}. It seemed very unlikely that the γ ray should come from $C^{12*} \longrightarrow Be^{8*}_{15\ \mathrm{Mev}} + \alpha$, since the lowest-energy state in C^{12} available to this reaction would be $7.374 + 15 \cong 22.4$ Mev and the probability of α emission would be strongly decreased, because C^{12} is unstable against neutron and proton emission at this excitation energy. The physical size of the pair spectrometer limited us in the early stages of the work to the use of the 184-inch synchrocyclotron, so that we were not able until later to use a threshold technique to make the determination.

We were, however, able to use a variety of reactions. The 15-Mev γ ray was observed with a carbon target for proton energies ranging from $\sim$30 to 340 Mev, but was not observed in the proton bombardment of Be, B, and 0. It was observed in the deuteron bombardment of natural boron(81% B^{11}), in which deuterons of 18, 30, and 50 Mev were incident on a thick target. It was not observed in the deuteron bombardment of a thick target of B^{10}. Referring to Fig. 1, we see that the reaction $B^{11} + d \rightarrow C^{12*} + n$ will excite levels in C^{12} above 13.734 Mev, and that the reaction $B^{11} + p \rightarrow C^{12*}$ will excite levels in C^{12} above 15.957 Mev. If the γ ray originated from the decay of a 15-Mev level in C^{12} we should expect to see the decay in $B^{11} + d$ and not in $B^{11} + p$, as the latter reaction would require the emission of a low-energy photon to the 15-Mev state followed by a transition to the ground state. On the other hand, if the 15-Mev level were in Be^{8}, we would expect a yield from the $B^{11} + p$ reaction as well as from $B^{11} + d$. The fact that we did see the γ ray from $B^{11} + d$ and not from $B^{11} + p$ further indicates that we were seeing the decay of a 15-Mev level in C^{12}.

After announcement that this gamma ray had been seen,[8] we received a communication from V. K. Rasmussen et al.[9] of Indiana University stating that they had verified the production of a 15-Mev gamma ray in the deuteron bombardment of B^{11}. They also observed the γ ray from the bombardment of a thick beryllium target by 21.7-Mev α particles. This fact suffices to prove that the radiation comes from an excited state in C^{12}, since a 15-Mev state in Be^{8} is not energetically accessible in the bombardment of Be^{9} with 21.7-Mev α particles (see Fig. 1).

Once it is established that the radiating level is in C^{12}, it is apparent that some selection rule must be operating to inhibit α emission. The decreased α width may be understood if we say that we are dealing with a state of isotopic spin T = 1. Both states in Be^{8} that are available through α decay are T = 0, and the He^{4} nucleus is also T = 0, so that requiring the conservation of isotopic spin in nuclear reactions forbids the[10,11] decay of a T = 1 level in C^{12} by α emission.

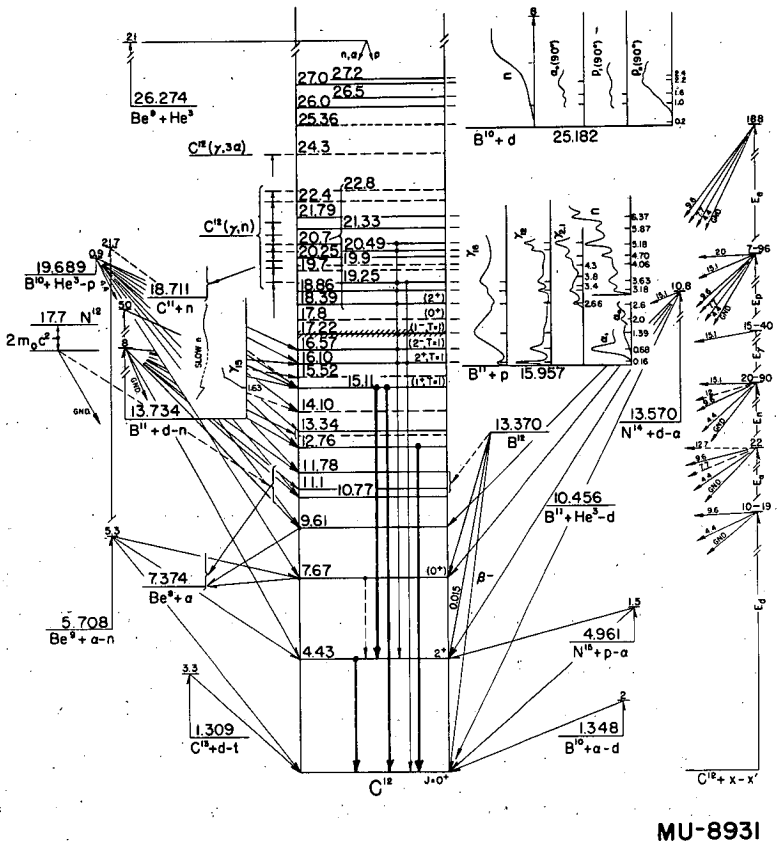

Fig. 1. Energy levels of carbon-12. The observed gamma rays are indicated by the heavy arrows.

The isobaric triplet having states of the same character would be B^{12}, C^{12*}, and N^{12}. The first T = 1 state in C^{12} is the analogue of the ground states of B^{12} and N^{12}, and calculations of its excitation energy yield 15.4 and 15.19 Mev.[12] These energies were obtained from the masses of B^{12} and N^{12} after correction for the neutron-proton mass difference and for the Coulomb energy difference between members of the isobaric set.

From this point on, the experiment was concerned with the following points:

(a) determination of the characteristics of the C^{12} level,

(b) the investigation of the role of conservation of isotopic spin in nuclear reactions, and

(c) the investigation of the mechanism for producing this excited state in nuclear reactions.

Additional data regarding the 15.1-Mev level have been reported since the publication of References 3 and 9. Barnes and Kavanagh report the measurement of the threshold for producing 15.1-Mev γ rays in the reaction $B^{11}(d, n)C^{12*}$.[13,14] The threshold for neutrons from the formation of this state from $B^{11}(d, n)C^{12*}$ has also been reported by Marion, Bonner, and Cook.[15] A proton group from $B^{10}(He^3, p)C^{12*}$ proceeding to a level at 15.1 ± 0.1 Mev has been found by Bigham, Allen, and Almqvist at Liverpool.[16] Further work on the reaction $B^{10}(He^3, p)C^{12*}$ in which coincidences have been measured between the 15.1-Mev gamma rays and the associated proton has been reported by Gove et al.[17] In addition Gove reports the observation of coincidences between gamma rays of 4.43 and 10.7 Mev corresponding to transitions from the 15.1-Mev level to the first excited state of C^{12}.[18] Fuller, Hayward, and Svantesson have observed elastic scattering of 15.1-Mev photons from C^{12} irradiated with bremsstrahlung from the NBS betatron.[19] Measurements of the attenuation produced when a carbon absorber is placed between the betatron and the scattering target, and of the absolute number of photons scattered, have been combined to yield values for Γ_t and $\Gamma_{\gamma 0}$.[20,21,22] Leiss and Wyckoff have measured the angular distribution of elastically scattered photons at NBS and find it to indicate the assignment of J = 1 for the 15.1-Mev level.[22] More complete reference to these data is made at appropriate places within the thesis.

II. INSTRUMENTATION

A. Magnetic Pair Spectrometer

A gamma ray of energy greater than $2\,mc^2$ can, in passing through material, interact with the Coulomb field of a nucleus and produce an electron-positron pair. Since the mass of the electrons is much smaller than the mass of the nucleus, the electron pair carries away most of the energy of the gamma ray and thus the center of gravity of the pair moves almost collinearly with the photon.[23] The measurement of the energies of the electron and the positron yields the energy of the initiating photon. The spectrometer used in these experiments performs a magnetic analysis of the pairs produced in a thin converter. A diagram of the apparatus is shown in Fig. 2, which is a horizontal cross section through the gap of a large magnet used to produce a magnetic field perpendicular to the plane of the paper.

The particles of the pair produced in the converter follow circular paths in the magnetic field. A fraction of the positrons will enter one of the ten geiger counters in the right bank, and similarly, a fraction of the electrons will enter one of the ten geiger counters on the left. Coincidences are observed between any one of the ten positron counters and any one of the ten electron counters giving, in all, 100 possible coincidence pairs. If a coincidence is observed between two counters whose separation is $2r$, then the sum of the radii of curvature of the positron and electron (r^+ and r^-) is equal to r. The momentum of an electron is proportional to Hr, so that the sum of the momenta of the positron and electron is

$$p^+ + p^- \propto H\,(r^+ + r^-) = H\,r.$$

The energy of the initiating photon is equal to the total energy of the pair, or

$$k = E^+ + E^- = (p_+^2 + \mu^2)^{1/2} + (p_-^2 + \mu^2)^{1/2} = p_+\left(1 + \frac{\mu^2}{p_+^2}\right)^{1/2} + p_-\left(1 + \frac{\mu^2}{p_-^2}\right)^{1/2}.$$

for

$$p^+ \gg \mu,\ p^- \gg \mu,\ \text{then}$$

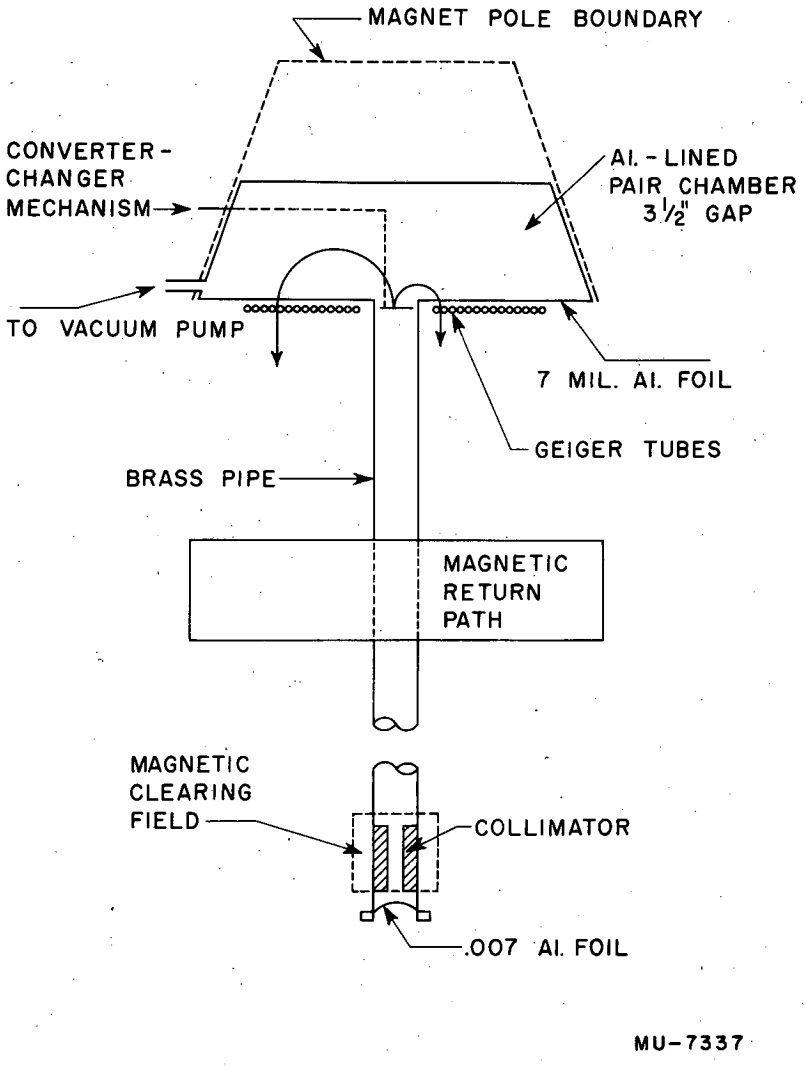

Fig. 2. Schematic view of the 19-channel pair spectrometer. The diagram shows a horizontal cross section through the gap of a large magnet used to produce a magnetic field perpendicular to the plane of the drawing.

$$k \approx p_+\left(1 + \frac{\mu^2}{2p_+^2}\right) + p_-\left(1 + \frac{\mu^2}{2p_-^2}\right)$$

$$\approx (p_+ + p_-)\left(1 + \frac{\mu^2}{2p_+p_-}\right),$$

$$k \propto Hr\left(1 + \frac{\mu^2}{2p_+p_-}\right).$$

The correction term $\mu^2/2p_+p_-$ depends upon the individual momenta, p^+ and p^-, and thus upon the particular pair of G-M tubes of spacing $2r$ that take part in the coincidence. We may calculate the correction term using the approximation $k \approx p_+ + p_-$. The correction for the pair of equidistant geiger tubes is

$$\frac{\mu^2}{2p_+p_-} \simeq \frac{\mu^2}{2(\frac{k}{2})(\frac{k}{2})} = \frac{2\mu^2}{k^2}.$$

The limiting case for the spectrometer used is $p_\pm = 0.7k$, $p_\mp = 0.3k$, for which the correction term is

$$\frac{\mu^2}{2p_+p_-} \simeq \frac{\mu^2}{2(0.7k)(0.3k)} = 2.38\ \frac{\mu^2}{k^2}.$$

Using the average of these two we may write

$$k \propto Hr\left[1 + 2.19\ \frac{\mu^2}{k^2}\right],$$

The pair spectrometer was designed for use in the 10- to 150-Mev energy range, and the correction term for a 10-Mev photon is 5.5×10^{-3}. This is very much smaller than the resolution of the spectrometer due to geiger tube width, so that we may write

$$k \propto Hr.$$

The above discussion indicates that in a uniform field, all pairs of counters having the same separation are sensitive to gamma rays of the same energy. It is of course necessary to verify that at any particular magnetic field setting the magnetic field remains sufficiently uniform that the electron or positron energy is proportional to r. This verification was made by use of the floating-wire technique.[1] The magnetic field was also calibrated absolutely at several points in the field, by use of a nuclear induction apparatus. An independent check

of the calibration was obtained by observing the 17.6-Mev gamma ray emitted by Be^{8*} produced in the reaction $Li^7 + p \rightarrow Be^{8*}$. [4,24] The agreement between the three calibrations was within the experimental errors.

A block diagram of the electronics used in the experiment is shown in Fig. 3. An electron-positron pair is detected by Geiger-Mueller tubes in both the left and right banks. The resulting G-M tube pulses are changed to 1 microsecond pulses in the pulse-forming unit and a coincidence is detected in the 10-channel quad mixer. If pulses from the left and right banks occur within the resolving time of $\sim$1 μsec, a gate signal is fed to the 35-channel gated amplifier. The two gated G-M tube pulses trigger one-shot multivibrators which produce 20-millisecond pulses suitable for actuating registers. These pulses are fed to the G-M registers, which monitor the coincident counting rate in individual G-M tubes, and to the 10-by-10 coincidence matrix, which is used to sum counts from pairs of G-M tubes of the same separation. The outputs from the matrix are recorded in the 29-channel registers.

Spurious counts can occur if

(a) counts from the left and right banks "accidentally" occur during the resolving time,

(b) a count appears on the left or right bank in coincidence with a true event; and

(c) two real events occur within the $\sim$10-msec resolving time of the 10-by-10 matrix.

The spurious counts were eliminated or subtracted as follows:

(a) The number of accidental counts was monitored with an identical coincidence circuit fed with the pulses from the left bank delayed with respect to those from the right bank. The resolving times of the two coincidence circuits were made equal through the use of a Berkeley double-pulse generator. The adjustments were checked by feeding random pulses into the left and right banks. The beam level was normally reduced to the point where the accidental ratio was $<10\%$. In order to obtain the accidental spectra, the output of

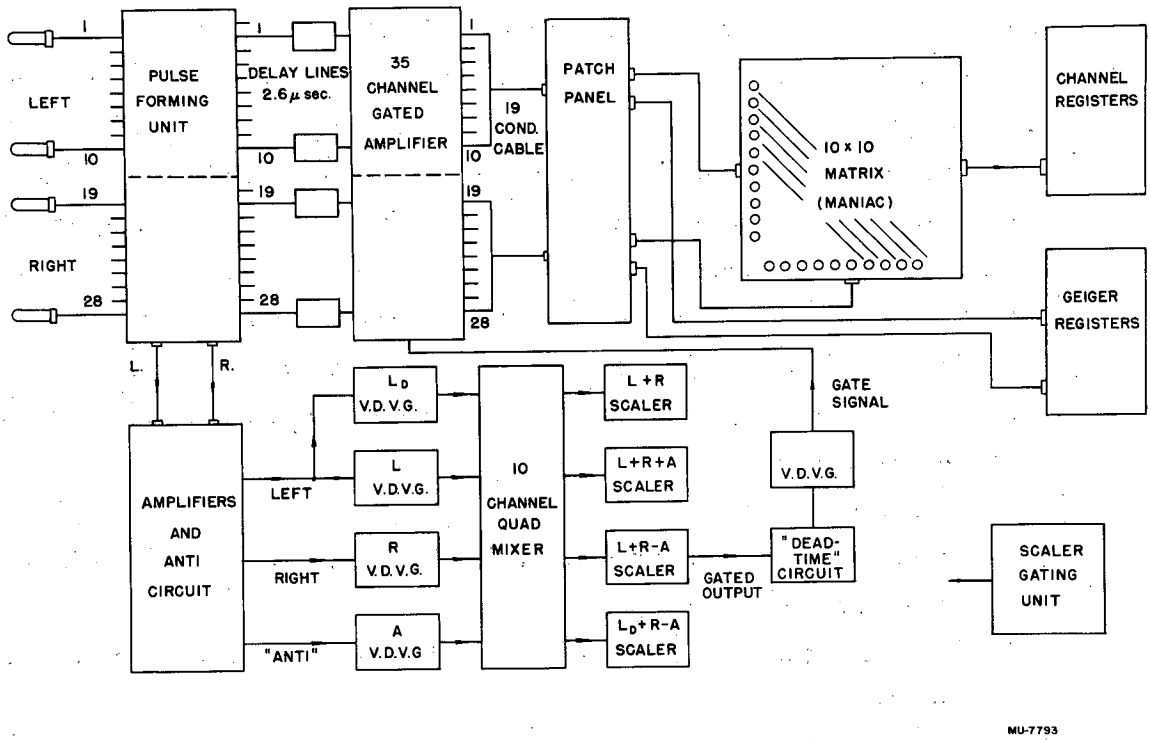

Fig. 3. Block diagram of pair-spectrometer electronics.

the scaler-gating unit was fed to the 35-channel gated amplifiers to permit recording the singles rates on the G-M tubes during the beam pulse. From these rates one can calculate the shape of the accidental spectra and normalize to the number of accidental counts during a run. This procedure substantially reduced the amount of beam time necessary to make a subtraction of accidentals.

(b) The output of the pulse-forming unit was designed to give an output pulse whose amplitude depends upon the number of G-M tubes firing within a 1 μsec resolving time. Thus, if a true left-and-right coincidence is accompanied by a spurious left count, the left output of the pulse-forming unit is of double height. A germanium diode discriminator circuit is then used to produce an "anti" pulse, which is put in anticoincidence with the true event. It can be seen that the relative probability that counts in any energy channel are suppressed through the action of the anticoincidence circuit is proportional to the counting rate in each energy channel. Thus, the elimination of these spurious events does not lead to a distortion of the measured spectrum. However, a scaler was used to monitor the number of left and right events so that the data could be corrected for those events that were eliminated by this circuit.

(c) If two separate coincidences are allowed to arrive at the matrix separated by less than $\sim$10 msec, then it can be seen that as many as four registers could record, giving two false counts. The dead-time circuit permits gates to be passed to the 35-channel gated amplifiers only if they are separated by more than 20 msec. As is indicated in the preceding section, the suppression of events that occur within the 20-msec dead time does not lead to distortion of the measured spectrum. However, as above, the numbers of gates before and after the dead-time circuits were recorded in order to correct the data for events that were eliminated. Under normal operating conditions, reducing the beam to the level where the accidental ratio was small also made the number of counts not registered negligible.

A more complete description of the electronics equipment is to be found in Reference 1.

The various factors that can contribute to the resolution of the spectrometer are the following:

1. The Finite Width of the Counters

The energy width of a channel is determined by the dimensions of the G-M counters. If only the size of the counters determined the line shape, we would obtain a triangular resolution function. That is, for a monoenergetic gamma ray, as the magnetic field is changed the counting rate in a single energy channel would be an isosceles triangle (Fig. 4). The base of the triangle would have a width

$$H_{max} - H_{min} = \frac{W}{r} H_0 ,$$

where W = width of G-M tubes, $2r$ is the separation of G-M tubes in a channel, and H_0 is the field for maximum counting rate. The counter separation is different for each of the output channels; the inner pair of G-M tubes (Channel 1) have $w/r = 0.16$ and the outer pair (Channel 19) have $w/r = 0.06$. Using an average value, we obtain the resolution at half maximum due to counter width alone as

$$\overline{\Delta H} \simeq \frac{\overline{W}}{2r} H_0 \simeq 0.05 H_0 .$$

It is important to note that when the magnetic field is fixed, the counts due to a monoenergetic gamma ray appear in two adjacent channels that overlap in energy.

2. The Angular Divergence of the Emitted Electrons

If either electron of a pair is emitted or scattered in any direction in which the horizontal component of motion does not lie along the normal to the converter it will appear to have too low an energy because of the property of 180° focusing. The result is to make the observed line shape asymmetrical, with a tail on the low-energy side (Fig. 5). If the vertical component of motion does not lie along the normal to the converter, it is possible for the emitted electron to miss the G-M tube, thus reducing the counting rate of the spectrometer. The correction for vertical scattering is the same, to first order, for all gamma rays measured at a fixed magnetic field.

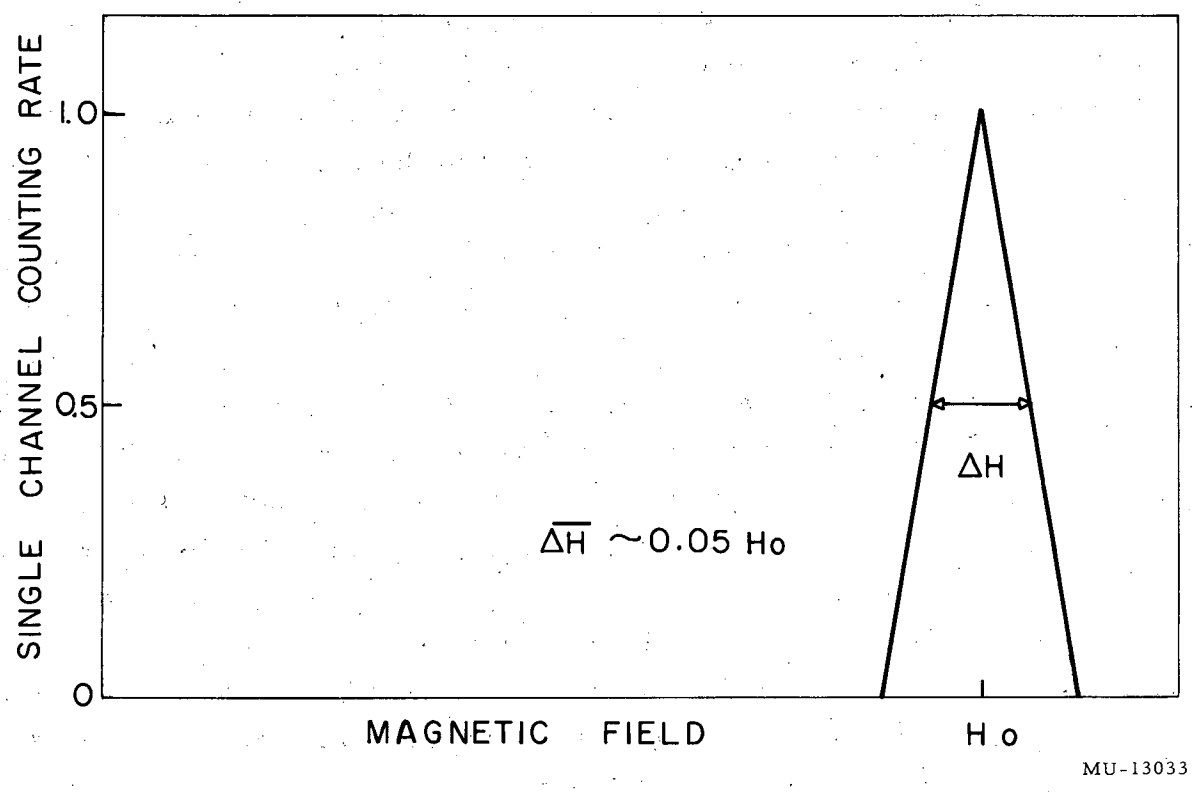

Fig. 4. Effect of Geiger-Mueller tube width on the line shape of the pair spectrometer.

The process of creating an electron-positron pair through the absorption of a gamma ray does not produce electrons along the direction of the incident photon, but rather gives a characteristic angular distribution for the electrons (see Appendix 1). In addition, the electrons can be scattered as they pass through the converter. The relative importance of these effects is governed by the thickness of the converter, because--for example--a very thin converter will not produce scattering, so that one need consider only the angular distribution obtained in the process of pair production. It is shown in Appendix 2 that multiple scattering of the electrons is the predominant mechanism operating for thicknesses of converters used in the spectrometer.

As is shown in Appendix 4, the counting rate, or efficiency, of the spectrometer is determined primarily by the vertical scattering, and the line shape is determined primarily by the horizontal scattering. Since the effect of 180° focusing is to reduce the apparent radius of curvature of an electron ejected with a horizontal component of scattering, horizontal scattering does affect the efficiency, or counting rate, of the spectrometer. A gamma ray that is being measured with a magnetic field setting such that the counting is being done in the lower energy channels will have a reduced counting rate, since the horizontally scattered electrons can have an apparent radius of curvature less than that of the innermost G-M tube. On the other hand, when a gamma ray is being measured in the higher-energy channels, the counting rate, or efficiency, will be increased by the scattering of electrons that would, in the absence of scattering, have radii of curvature too large for the outermost G-M tubes and that can, after scattering, enter the sensitive area of the spectrometer and be counted. This effect changes the relative efficiencies, or counting rates, of the lower- and higher-energy channels.

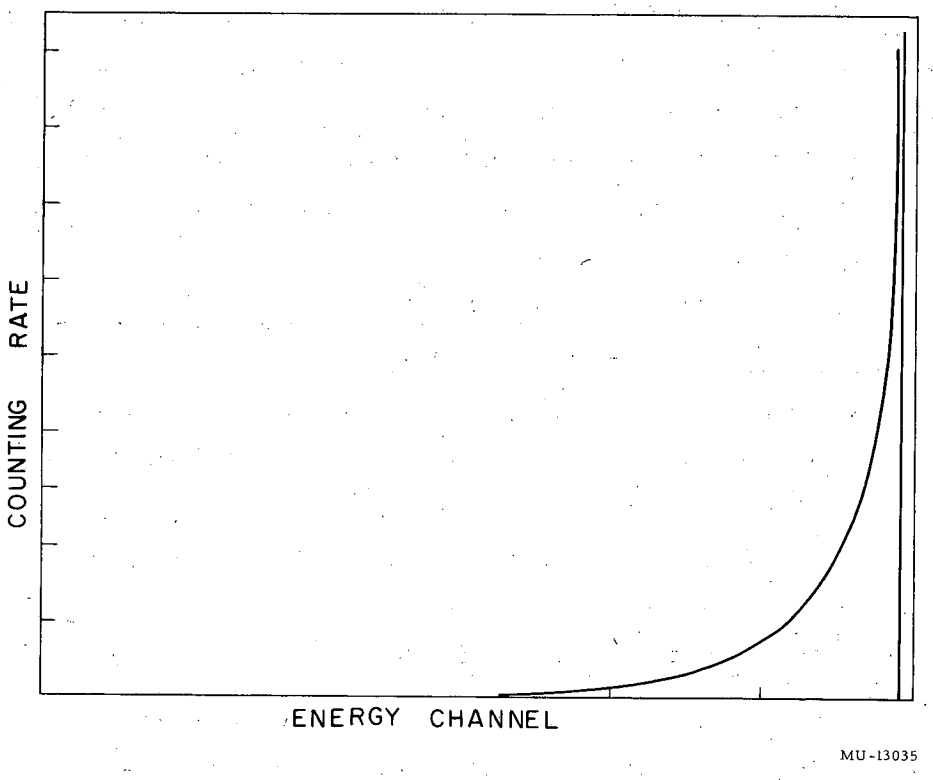

Fig. 5. Effect of multiple scattering of electrons in the converter on the line shape of the pair spectrometer.

3. Scattering of Electrons by Pole Faces and Foil in Front of Counters

Because of scattering the edge of a counter is not sharply defined as far as the electrons are concerned. Any effect observed as a result of these scatterings should be approximately symmetrical on the high- and low-energy sides. For a 5-Mev electron, the effect of the foil is to increase the width of the G-M tube by $\sim$1%, which is insignificant with regard to resolution and efficiency. The electrons that strike the pole faces, and which may subsequently be scattered, are those that have experienced a sufficient amount of vertical scattering in the converter to cause them to miss the G-M tubes. Thus using a thin converter to reduce scattering loss also minimizes line-shape distortion due to scattering from the pole faces. In addition, the pole faces were lined with aluminum to reduce the fraction of incident electrons that scatter into the G-M tubes.

4. Deviations from Normal Incidence of Gamma Rays Striking the Converter Far from its Center.

The effect of angular divergence arising from nonnormal incidence of gamma rays on the converter is to lower the observed energy of a gamma ray. Because the distance from the target to the converter is large ($\sim$ 40 ft at the cyclotron, 15 ft at the linac) compared with the width of the converter (2.5 inches), this effect is negligible.

5. Energy Loss by Electrons in the Converter

Loss of energy through collisions by the electrons in the converter causes the peak to shift toward lower energies by just the amount of the average energy loss (Appendix 2). In addition to shifting the position, energy loss in the converter also produces a small loss in resolution. This arises from the fact that electrons traverse thicknesses of the converter ranging from zero to the full thickness (Fig. 6). This factor was taken into account in the computation of the line shape and efficiency of the spectrometer, but it is small compared with the effect of multiple scattering.

Energy loss due to radiation tends to make the shape of a gamma line asymmetrical, with a tail on the low-energy side, rather than to shift the position of the peak (Fig. 7). However, observation with an instrument of finite resolution results in appearance of the maximum counting rate in a lower-energy channel. In Appendix 3 it is shown that the effect of radiation straggling is small compared with multiple scattering, for converter thicknesses used in this experiment. It is interesting to note that the processes of pair production, bremsstrahlung, and multiple scattering vary as Z^2 (i.e., as the number of radiation lengths), whereas collision loss depends upon Z. Thus choice of a converter material does not affect the relative importance of the first three processes, but the last process may be reduced in importance through the choice of high-Z material. For this reason, Ta was used as the converter material as a compromise between high Z and suitable physical properties.

6. Misalignment of the Converter

If the pair is produced at a position not in line with the G-M tubes, the focusing property of the 180° geometry reduces the apparent energy of the gamma ray. The fact that proper focusing was obtained in the plane of the G-M tubes was verified during the calibration of the spectrometer, using the wire-orbit method. The phenomenon of energy reduction was manifested during the first run with the new converter changer when it was observed that the energy of the 15-Mev gamma ray had shifted downward. Investigation showed that eddy currents produced in the frame of the holder during the changing of the magnetic field had shifted the position of the converter. Thenceforth the position of the converter was checked following each change in magnetic field.

7. Pairs Produced in the Chamber.

As with converter misalignment, pairs not produced in the converter foil result in the observation of a gamma ray of reduced energy. This effect is eliminated by careful collimation and alignment. To test the alignment, a dummy converter holder was used to make a converter-out subtraction. It was found that, for most runs, the counting rates with the converter removed was equal to the accidental rate.

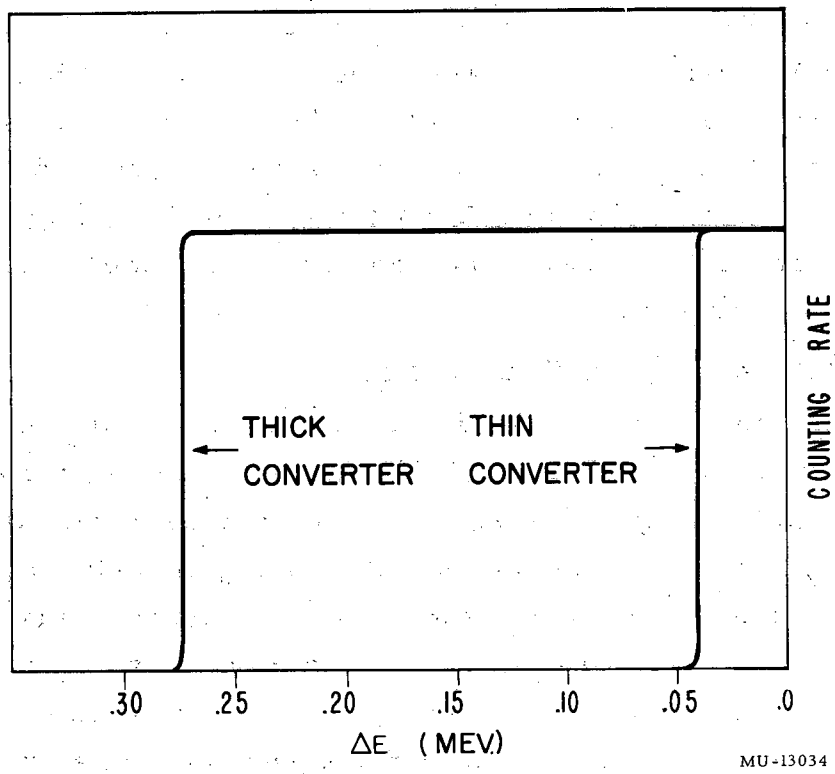

Fig. 6. Effect of energy loss by the electrons through collisions in the converter on the line shape of the pair spectrometer.

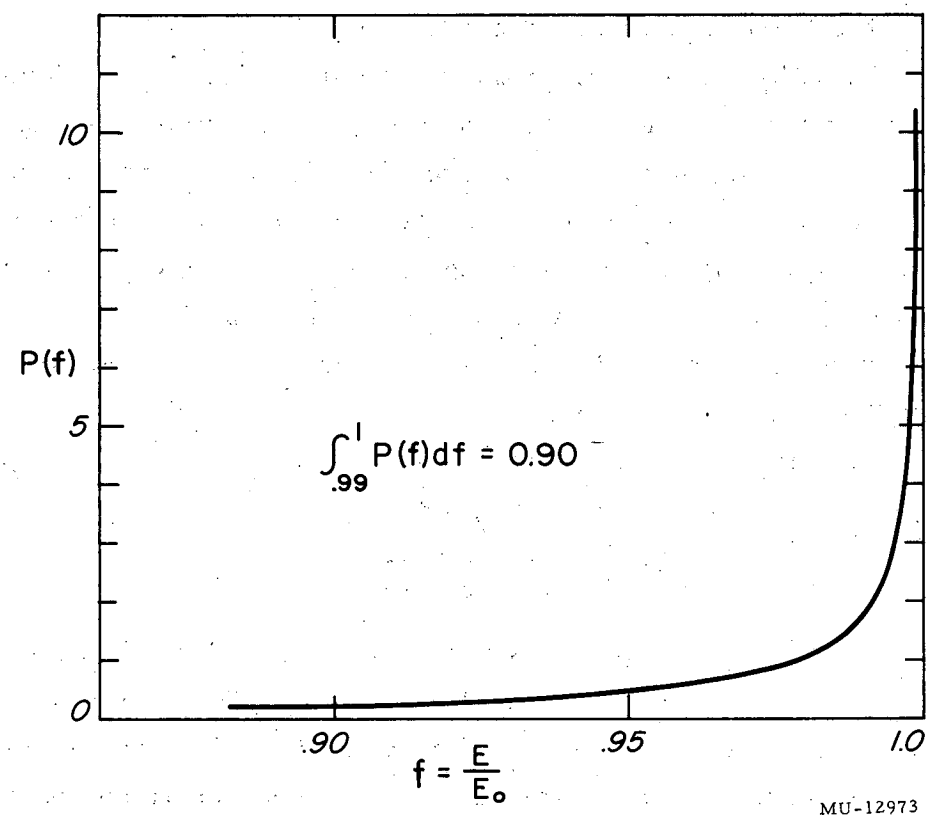

Fig. 7. Effect on the line shape of the pair spectrometer because of energy loss by the electrons through radiative collisions in the converter.

B. NaI(Tl) Crystal

The technique of gamma-ray spectroscopy using scintillation counters with thallium-activated sodium iodide as a scintillation phosphor, as introduced by Hofstadter,[26] is well known, and several reviews on the subject have been written.[27, 28, 29, 30, 31] Gamma rays interact with the phosphor by three principal processes—Compton scattering, photoelectric effect, and pair production. Tables of the cross sections for these processes for different materials have been calculated and are available for calculations of efficiency.[32, 33]

In order to determine the total number of interactions occurring in the crystal it is necessary to know the expected pulse-height distributions for gamma rays of different energies in a crystal of given dimensions. If we consider only primary interactions, the photoelectric effect gives a "line" spectrum corresponding to the full energy of the gamma ray, assuming that no x-rays escape from the crystal. The Compton effect gives rise to a broad distribution of pulse heights corresponding to the energies of the recoiling electrons. This distribution has a sharp upper limit resulting from an electron of energy

$$E_{max} = \frac{2E_\gamma^2}{(2E_\gamma + mc^2)}$$

The pair-production process gives rise to a "line" at an energy $E = h\nu - 2\,mc^2$ resulting from the energy loss of the electron-positron pair. The observed spectra differ considerably from those expected on the basis of primary interactions only. The additional factors affecting the spectra are:

(a) The finite resolution of the crystal-photomultiplier system--arising from the statistics of light production and light-collection efficiency, photocathode efficiency and photoelectron collector efficiency, nonuniformity of the photocathode, and the process of photoelectron multiplication--broadens the distributions obtained for gamma rays of all energies.

(b) The x-rays produced after photoelectric effect can escape from a small crystal and produce an escape peak of energy $E = h\nu - E_{K,L}$,

where $E_{K,L}$ is the binding energy of the K or L electron in iodine.

(c) The photons scattered in Compton effect may be captured in the crystal and produce a pulse corresponding to the full energy of the gamma ray.

(d) The positron formed in pair production will annihilate with an electron and result in the production of two 0.51-Mev gamma rays. Thus we may have three different peaks in the spectrum corresponding to the absorption of none, one or both of the emitted photons. The separation between each of these peaks is 0.51 Mev, and the separation can be used as a check on the energy calibration.

(e) For higher-energy gamma rays the resulting electrons may escape from the sides and the ends of the crystal. This effect causes the line shape to be asymmetrical, with a tail on the low-energy side.

(f) High-energy electrons can also interact with the nuclei of the crystal and lose energy from the production of bremsstrahlung. Some of the resulting photons escape from the crystal and cause an asymmetrical line shape with a tail on the low-energy side.

It is readily seen that the effect of these secondary processes is very strongly affected by the size of the crystal used. Secondary photons (Compton, annihilation, or bremsstrahlung) produced in the center of the crystal have a higher probability of being captured in the crystal than those produced on the periphery. Similarly the probability that an electron will scatter from the side is determined by the position at which it originates. For these reasons, the incident gamma rays were collimated along the crystal axis. The crystal used in these measurements was a right circular cylinder 3 in. in diameter and 3 in. long, and was manufactured by the Harshaw Chemical Company. The collimators used had a 1-in. circular aperture and were 8 or 10 in. long. It was readily apparent that the collimation resulted in more easily resolved pulse-height spectra for higher-energy photons. The pulse-height distributions expected for higher-energy photons have been calculated and observed by several authors.[34, 35, 36, 37]

In order to use the NaI(Tl) crystal as a gamma-ray spectrometer it is necessary to establish a relationship between pulse height and the energy of the initiating gamma ray. This is accomplished by using

sources producing gamma rays of known energy and extrapolating this relationship between pulse height and energy into the desired region. In the measurements of gamma rays emitted from the excited states of the C^{12} nucleus it has been very convenient to use a PoBe neutron source, as it yields a 4.43-Mev gamma ray originating from the first excited state of C^{12} produced in the reaction $Be^{9}(\alpha, n)C^{12*}$. It has been established that the pulse height per Mev lost is very nearly independent of electron energy for a NaI(Tl) crystal,[31] therefore a linear extrapolation of energy can be used. However, it is essential to ascertain that the associated electronic equipment does not destroy this linear relationship. A calibrated pulser was substituted for the output of the photomultiplier when the pulse-height analyzer was set up. This procedure cancels any effects of nonlinearity in the associated amplifiers. It is possible to check over-all linearity by observing gamma rays of different energies from various sources. This procedure is satisfactory for gamma rays of a few Mev but forces one to make a rather large extrapolation to gamma rays of 15 to 20 Mev. In order to determine that IR drop in the voltage divider did not contribute to nonlinearity at higher energies, the voltage across the dynode structure was increased until the output pulse for a 4.43-Mev gamma ray was greater than that corresponding to 25 Mev. In order to keep the photoelectron collection efficiency constant, a constant voltage was maintained between the photocathode and the first dynode. Recalibration at this increased gain assured that any error in extrapolation would arise from processes within the crystal. Comparison of the output pulses from the 4.43-Mev and 15.1-Mev gamma rays indicated linearity of the NaI(Tl) crystal within the errors of measurement.

The UCRL ten-channel pulse-height analyzer[38] was used to obtain the pulse-height spectra. A ten-channel PHA does not permit one to measure an entire spectrum at one time, so that it is necessary to change the relationship between the pulse height and the settings of the analyzer. It was found that nonlinearity of the linear amplifiers made it undesirable to use a subtractor, since it was necessary to readjust the discriminator settings each time such a change was made. As a result,

it was decided to leave the analyzer settings fixed and to change the amplitude of the input signal by means of an attenuator. This technique has the advantage that the fractional resoltuion (window width/pulse height) is the same for all portions of the spectrum. An additional advantage is that one is able to keep track of the relative widths of the channels by using a sliding pulser and quickly observe any drifts in the discriminator circuits or linear amplifier.

Nonuniform photosensitivity across the cathode surface produces different pulse heights for flashes occurring in the phosphor near regions of high and low sensitivty.[31] This effect was reduced by placing a light pipe between the crystal and the photomultiplier to distribute the light more evenly across the photocathode. Optical coupling between surfaces was achieved through the use of Dow-Corning DC-200 silicone oil. A Du Mont K-1197 (prototype of 6363) end-window photomultiplier was used. To achieve maximum collection of photoelectrons the voltage between the photocathode and first dynode was set at 300 volts and the potential of the auxiliary focus electrode was adjusted to obtain the largest output pulse.[31] To reduce photomultiplier noise the outside of the photomultiplier was painted with silver paint, which was in turn electrically connected to the photocathode and the case of the NaI(Tl) crystal. The photomultiplier was magnetically shielded with a mu-metal shield that extended past the photocathode and over the light pipe. This assembly was mounted inside two concentric soft iron cylindrical shields.

III. EXPERIMENTAL PROCEDURES AND RESULTS

A. High-Energy Excitation Function

The variation in yield of the 15.1-Mev level as the incident energy of protons bombarding a carbon target was varied from 60 to 340 Mev was measured at the 184-inch synchrocylotron. The physical arrangement of the experiment is shown in Fig. 8. The pair spectrometer viewed the carbon target at 90^{o} with respect to the direction of the internal beam. The targets were clamped to the end of a thin copper bar which was extended radially into the cyclotron-tank and the entire unit was bolted to the water-cooled end of the hollow probe. (see Fig. 9). Constantan wires soldered to both ends of the copper bar permitted measurement of the temperature difference resulting from the flow of heat down the copper bar. The thermocouple arrangement was calibrated by substituting a resistor for the target and measuring the differential emf for various input power levels. Under conditions of bombardment the power dissipated in the target is related to the amount of beam striking the target, and allows the determination of an absolute cross section.

The energy of the incident protons was changed by placing the target at different radii and using the known magnetic field to calculate the energy of the incident protons. Correction was made for the fact that the target-to-detector distance varied with each new setting of the target.

Figure 10 shows the photon spectrum obtained with the target placed at the 340-Mev radius. Here we can observe the photons arising from three different processes: (a) the higher-energy photons (peak $\sim$60 Mev) produced by the decay of the neutral π meson,[39, 40, 41], (b) the 15.1-Mev photons arising from the decay of the corresponding excited state of C^{12}, and (c) the lower-energy photons (falling continuum) produced by proton bremsstrahlung.[1] Figure 11 shows the change in photon spectrum as the energy of incident proton is lowered to 60 Mev. Reference to Fig. 14 indicates that the intensity of the 15.1-Mev gamma ray is not changing greatly over this energy region,

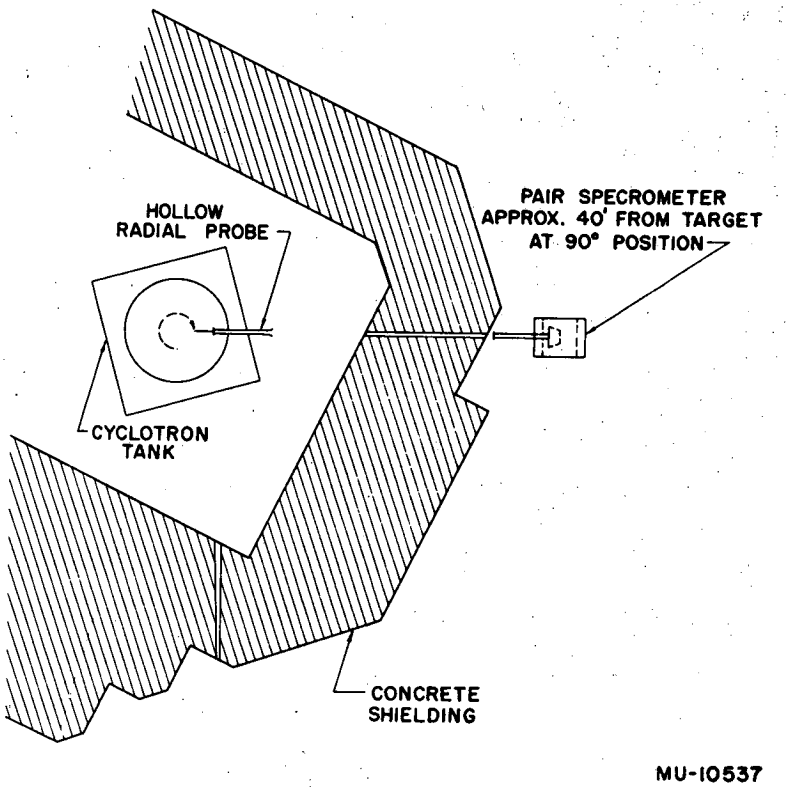

Fig. 8. Experimental arrangement at the 184-in. synchrocyclotron.

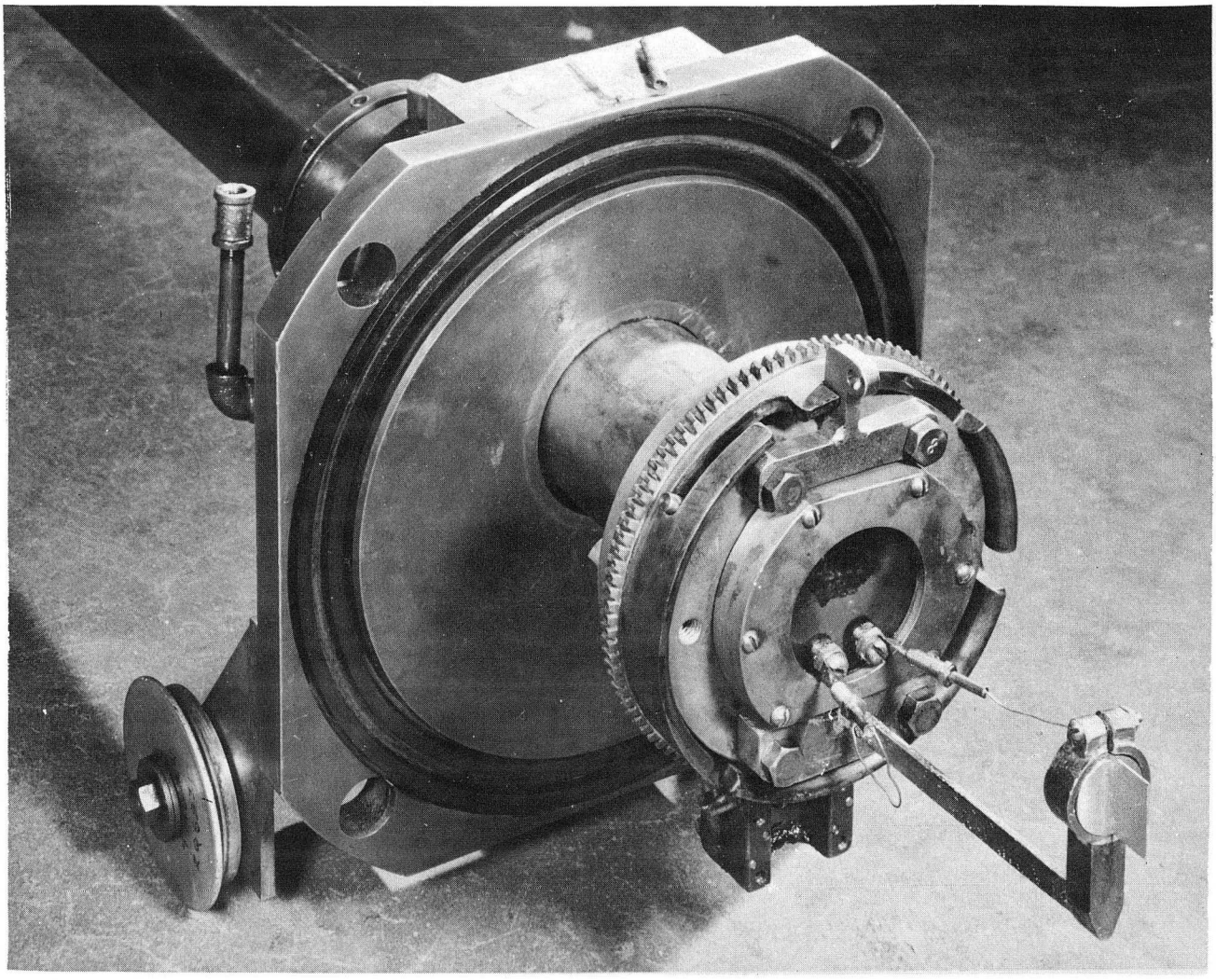

ZN-1410

Fig. 9. View of the target holder and thermocouple beam monitor. Constantan wires soldered to both ends of the copper bar permit measurement of the temperature difference arising from the flow of heat.

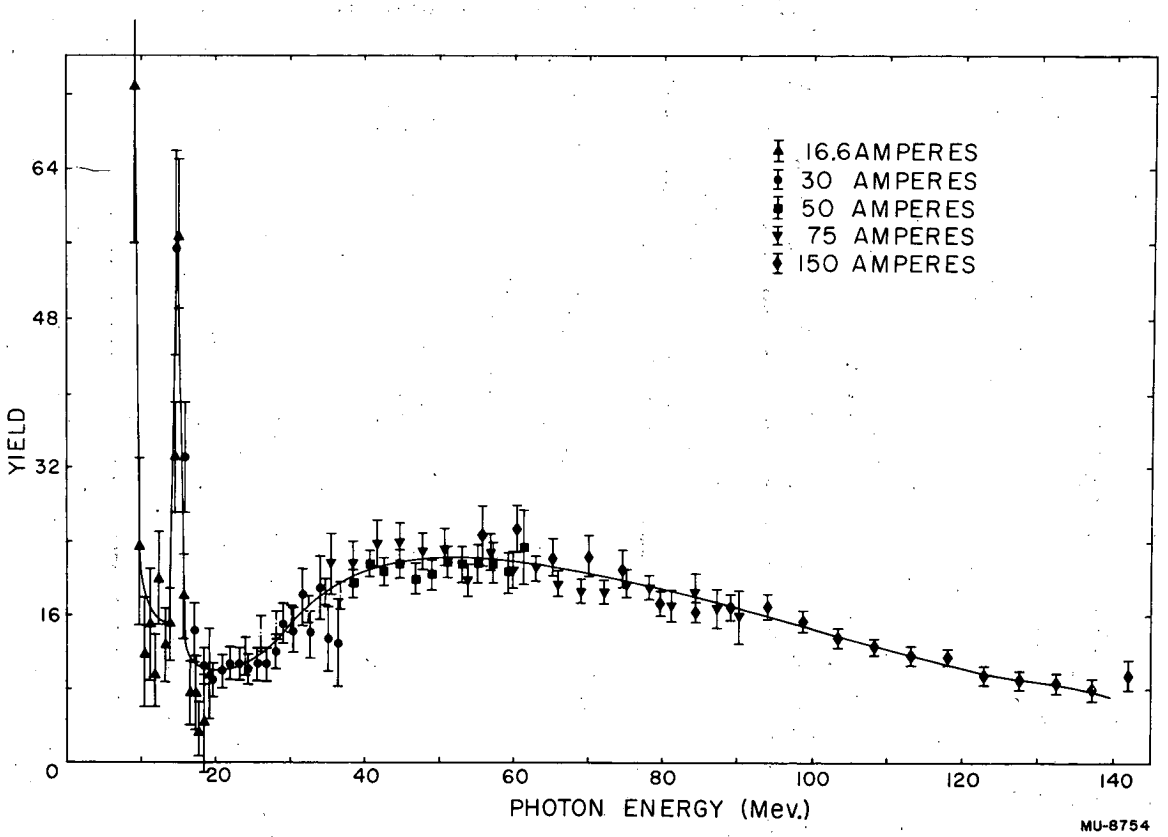

Fig. 10. Photon spectrum from the bombardment of a carbon target by 340-Mev protons. The photons are produced by three different processes:
(a) the higher-energy photons from the decay of the neutral π-meson, (b) the 15.1-Mev photons from the decay of the 15.1-Mev level of C^{12}, and (c) the lower-energy photons by proton bremsstrahlung.

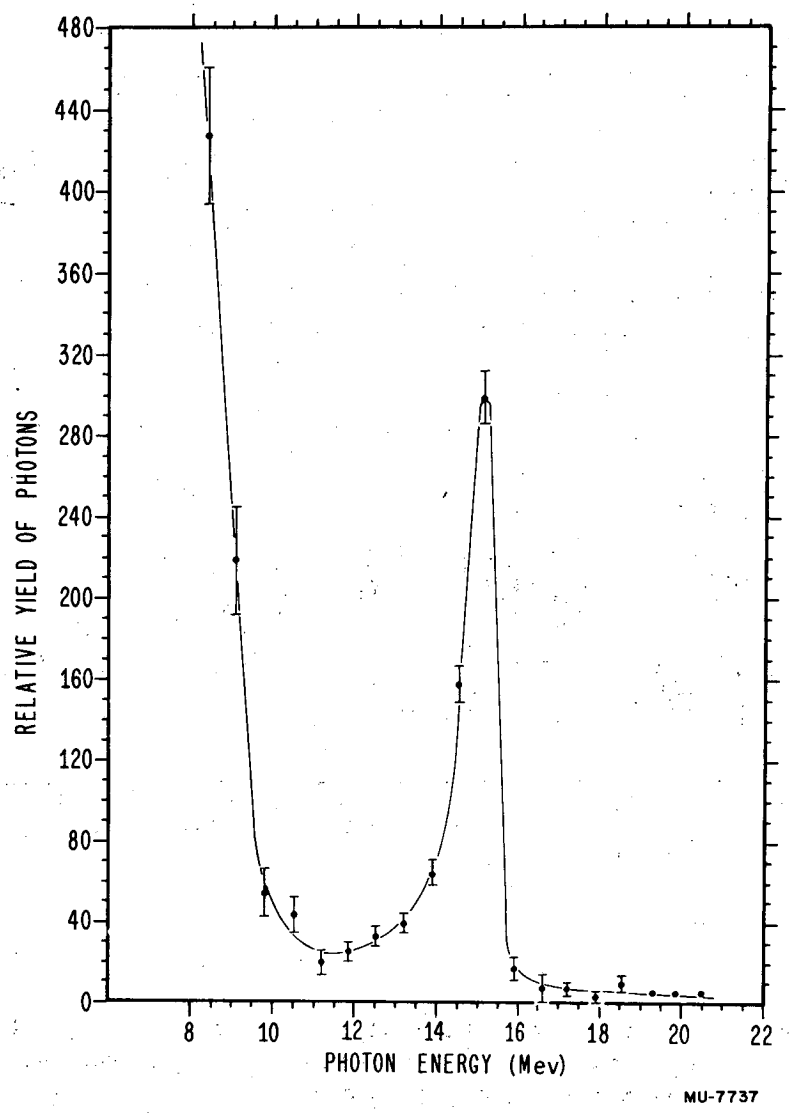

Fig. 11. Photon spectrum from the bombardment of a carbon target by 60-Mev protons. The photons arising from the decay of the 15.1-Mev level of C^{12} appear superimposed on the proton bremsstrahlung.

so that the change in spectrum shape arises principally from the variation in the intensity of the proton bremsstrahlung and elimination of π^0 photons as the incident proton energy is reduced.[1] The primary reason for measuring an excitation function for the production of an excited state of a nucleus over such an energy region was to try to get some insight into the processes involved in these higher-energy reactions.

Serber has pointed out that when a nucleus is bombarded by a high-energy nucleon the collision time between the incident particle and a particle in the nucleus is short compared with the time between collisions of the particles in the nucleus.[42] This leads to a picture of nuclear reactions in which the first step is the collision of the incident particle with the individual particles of the nucleus. At these energies the total cross sections for free nucleon-nucleon scattering have decreased to the extent that the mean free path for a nuclear collision is comparable to the size of the nucleus, and the nucleus begins to be transparent to the incident particles. In addition, the incident particle loses only a small fraction of its energy to the struck one. This implies that the collisions made by the incident particle cannot be considered as collisions between free particles, since it is impossible to leave the struck nucleon in a momentum state already occupied by some other nucleon of the nucleus. The result of this effect is to increase the mean free path of a high-energy particle traversing nuclear matter over that expected for collisions between free particles.

By use of this model of the nuclear reaction, it has been possible to compute an expected energy dependence for the production of the 15.1-Mev level in C^{12} by high-energy protons. It was assumed that the residual nucleus was excited through the collision of the incident proton with one nucleon that gained 15.1 Mev of kinetic energy. The probability of excitation through multiple collisions is assumed to be relatively small, since small momentum transfers are discouraged as a consequence of the approximate Fermi degeneracy of nuclear matter. Figure 12 shows the relative probability, as a function of incident proton energy, that a 15.1-Mev neutron will emerge from a free neutron-proton collision, and that a 15.1-Mev proton will emerge from a free proton-proton collision. The experimental values of $\frac{d\sigma}{d\omega}$ used in

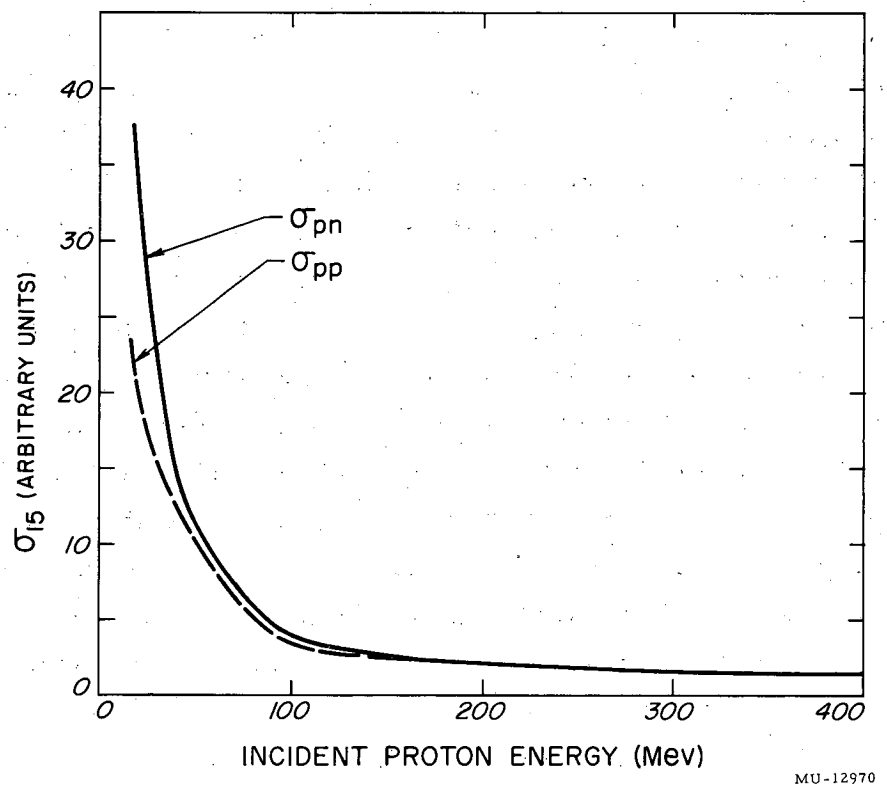

Fig. 12. Relative probability that a nucleon of 15.1-Mev will emerge from a free n-p and p-p collision. The experimental data come from the compilation by W. Hess.[43]

this calculation come from the compilation by Wilmot N. Hess of High-Energy Nucleon-Nucleon Cross-Section data.[43]

The mean free path of the proton in nuclear matter is given by

$$\lambda_t = \frac{1}{\langle \sigma f \rangle \rho},$$

where ρ is the nucleon density, σ is the total cross section for nucleon-nucleon collision, and f is a reduction factor attributable to the exclusion principle.[44] The brackets indicate an average over all the momentum states of the nucleons in the target. Figure 13 shows the calculated values for λ_t. Here we have taken

$$\bar{\sigma} = \frac{Z\sigma_{pp} + (A-Z)\sigma_{pn}}{A} = \frac{1}{2}(\sigma_{pp} + \sigma_{pn})$$

for C^{12}. The experimental values for the total cross sections were taken from Hess. The values of f were taken from Goldberger[45] and Morrison, et al.[46] who used a Fermi gas model to describe the nuclear states.

The probability that there is a single collision in a distance S that results in a 15-Mev nucleon is given by

$$P_1 = \int_0^S \left(e^{-\frac{x}{\lambda_t}}\right)\left(\frac{dx}{\lambda_{15}}\right)\left(e^{-\frac{S-x}{\lambda_t}}\right) = \frac{S}{\lambda_{15}} e^{-\frac{S}{\lambda_t}},$$

where λ_t = mean free path for all collisions,
and λ_{15} = mean free path for "15-Mev collisions."
The first term in the integral is the probability that there is no collision in the distance X, the second term is the probability that there will be a collision resulting in a 15-Mev nucleon in dx, and the last term is the probability that there is no collision in the remaining distance.

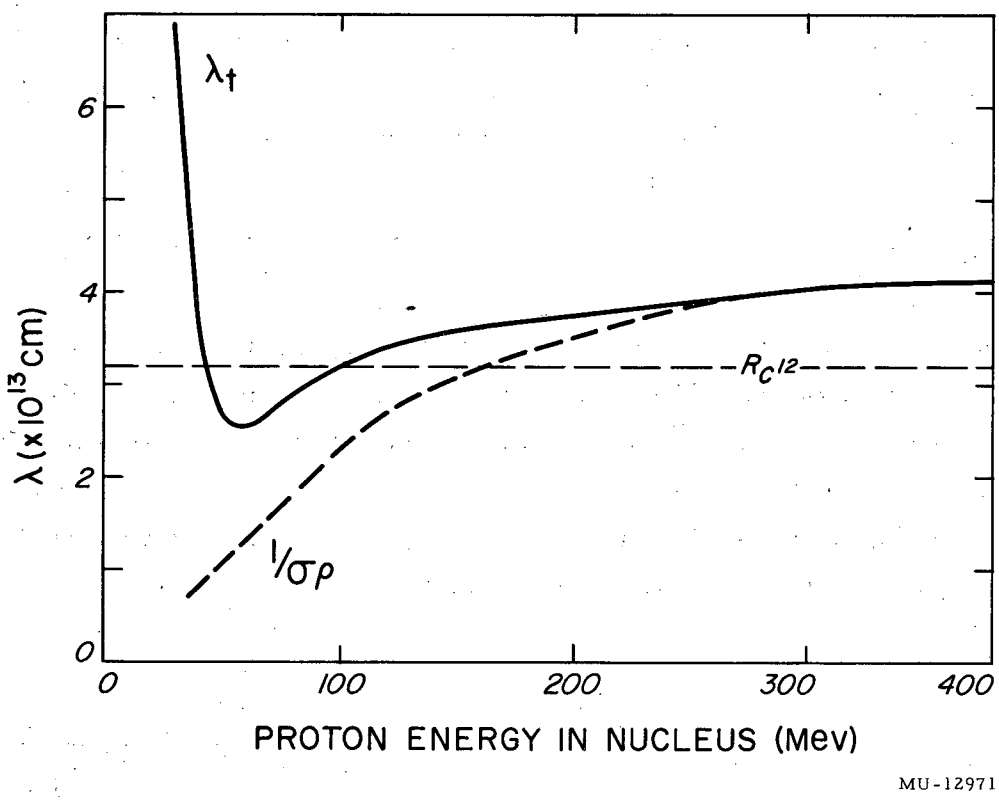

Fig. 13. Mean free path of a proton in nuclear matter.

Following the procedure of Fernbach, Serber, and Taylor,[47] we may calculate the cross section for a spherical nucleus. A particle passing through a sphere at a distance ρ from a line through the center emerges after traveling a distance $2S$, with $S^2 = R^2 - \rho^2$. Integrating the probability for a single collision over the sphere, we obtain

$$\sigma = 2\pi \int_0^R \frac{2S}{\lambda_{15}} e^{-\frac{2S}{\lambda_t}} \rho d\rho$$

$$= \frac{\pi \lambda t}{\lambda_{15}} \left[\lambda_t^2 - e^{-\frac{2R}{\lambda_t}} (\lambda_t^2 + 2R\lambda_t + 2R^2) \right] ,$$

$$\sigma \propto \sigma_{15} \left\{ \lambda_t \left[\lambda_t^2 - e^{-\frac{2R}{\lambda_t}} (\lambda_t^2 + 2R\lambda + 2R^2) \right] \right. .$$

The resultant excitation function is shown in Fig. 14 together with the experimental points that have been normalized to obtain the best agreement with the higher-energy points.

The agreement between the data and the calculated excitation function is better than should be expected in view of the simplifying assumptions made. Carrying the calculation to lower energies requires the consideration of refraction at the nuclear boundary and of barrier penetration for both ingoing and outgoing protons.[7, 48, 49] Experiments at 31 Mev seem to indicate that excitation occurs more strongly through interactions at the rim of the nucleus.[49, 50, 51, 52] As a result, the measured angular distributions have been compared with the theory of Austern-Butler-McManus, which considers interaction to occur only in the outer rim of the nucleus.[53]

The experimental variation of the cross section as the bombarding energy is changed has been reproduced rather well by the theoretical curve based on the assumption that the relative cross sections for nucleon-nucleon collisions within the nucleus are the same as for free nucleon-nucleon collisions. However, the absolute cross section for

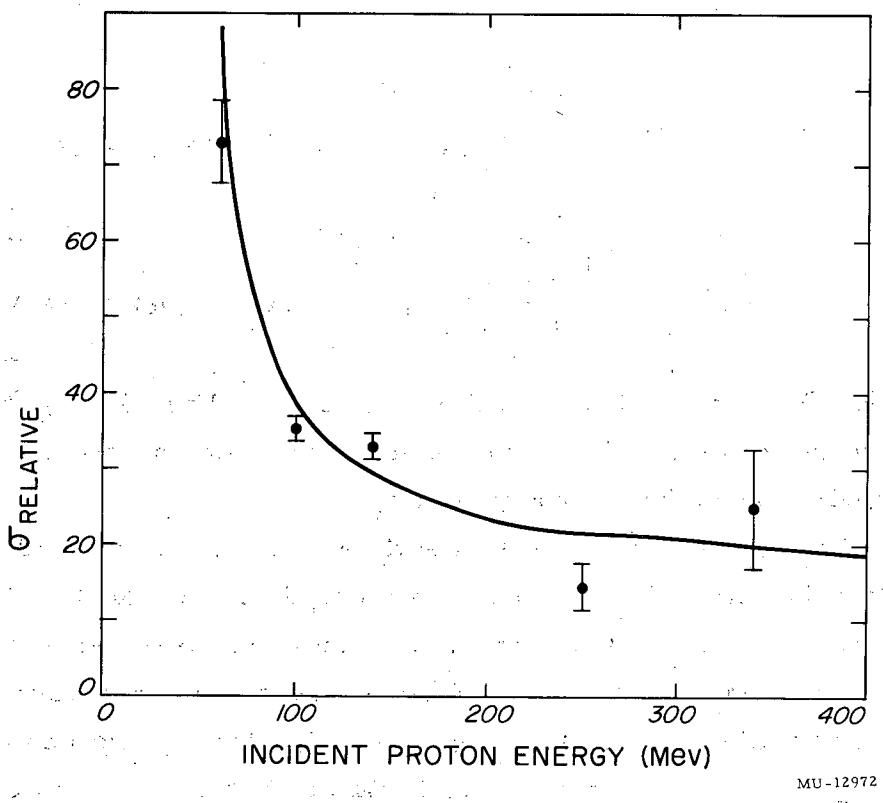

Fig. 14. Theoretical excitation function and normalized experimental data for $C^{12}(p,p')\,C^{12*}$ 15.1 .

producing an excited state via this mechanism depends upon the properties of the final state, i.e., upon the probability that the struck nucleon can form the excited state. This would argue that states that can be reached by a single-particle transition would be excited more strongly than states requiring the transition of two or more particles. Such an argument has been made by Strauch and Titus[54] and used to suggest the possible configuration of the 9.6-Mev state in C^{12}.

B. Low-Energy Excitation Function

The variation in yield of 15.1-Mev gamma rays as a function of incident proton energy from threshold to 31.5 Mev was measured while the pair spectrometer was at the linac. The energy of the incident beam was reduced by placing polyethylene absorbers in the beam prior to final collimation. Polyethylene was chosen so that the production of neutrons might be minimized. A 100 mg/cm^2 polyethylene target was used for all runs. Multiple scattering of the beam resulted in a reduction of the amount of beam collected in the Faraday cup as the energy of the protons incident upon the target was reduced. Correction for this effect was made by measuring the fraction of incident beam current that was lost when the target was placed in the beam. The largest fraction lost was 12%. Interpolation between measurements was made by assuming a Gaussian angular distribution[55] and using the fact that the rms angle of scattering is inversely proportional to the incident energy.

The Faraday cup was lined with carbon to reduce the neutron background and was made with a large aperture so that the reduction in the collection of beam when the target was placed in the beam would be small. Because of the large aperture no clearing field was provided, and therefore it was necessary to evaluate the effect due to secondary electrons in order to measure an absolute cross section. This measurement was made in collaboration with H. B. Knowles, who later used the same cup. Two measurements of this effect were made. The first consisted simply of comparing the relative beam currents measured by this cup and by the cup normally used at the linac. The beam was monitored by measuring

the protons scattered from a thin carbon target in the scattering chamber. Runs were made at varying beam intensities to assure that the monitoring counter was giving a true measurement of the integrated beam. The second measurement consisted of putting the Faraday cup in the magnetic field produced by a set of Helmholtz coils and observing the beam collection as a function of magnetic field. The beam was monitored by the scattered protons as before. As expected, the measured current attained a plateau for field strengths larger than that required to clear the electrons ejected from the front foil. Both measurements agreed within the errors associated with the measurements, and indicated that the measured current was 88.55± 0.53% of the actual current.

The excitation function obtained at the linac is shown in Fig. 15. We first note that the threshold is appropriate to the direct production of the 15.1-Mev state. The two points in which the energy of the protons dropped below threshold (shown partially dashed) have been corrected for the fraction of the target that takes part in the production of the 15.1-Mev gamma rays. Also shown are the thresholds for the competing reactions that originate in this energy region.

The process by which the carbon nucleus is excited by inelastic proton scattering in this energy region is still a subject for investigation. It is possible to consider that the reaction occurs through the formation of a compound nucleus (N^{13}) which lasts long enough for the incident proton to share its energy with all the nucleons.[56] A proton will be emitted when the energy imparted to it is sufficiently great that it can escape the nuclear well and penetrate the Coulomb and centrifugal barriers. Calculations have also been made in much the same manner as was done in Section III-A, assuming that the excitation is due to knock-on processes taking place throughout the whole nuclear volume.[48,49]

The Austern-Butler-McManus theory[53] involves the direct interaction of nucleons occurring in the peripheral region of the nucleus, and predicts angular distributions that are determined by the change in angular momentum of the proton.

However, regardless of the postulated interaction mechanism, there are features common to all that come from the fact that one can

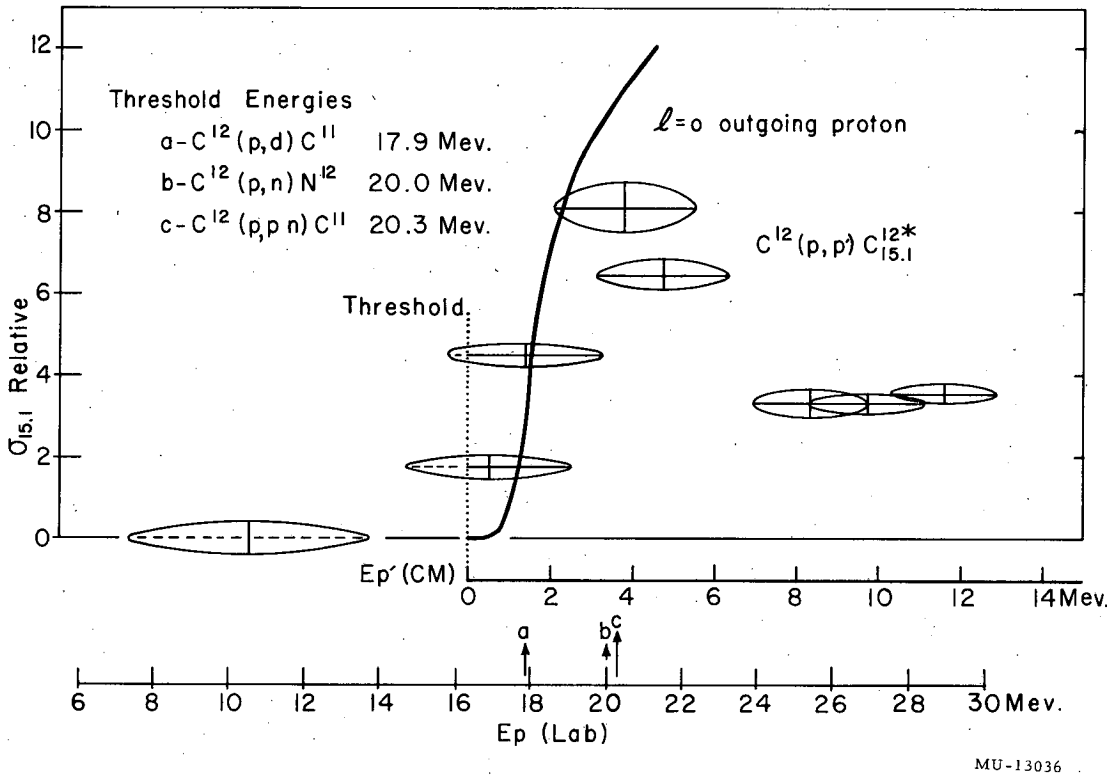

Fig. 15. Experimental excitation function for $C^{12}(p, p')C^{12*}$ 15.1 at lower proton energies. The thresholds for competing reactions that originate in this energy region are indicated. The expected energy dependence for an $l = 0$ outgoing proton is also shown.

with some exactness separate regions in which the Hamiltonian is fully known from regions in which it is not.[57] The known regions give the dependence of a reaction upon barrier penetration and reflection at the surface of the nucleus. This separation of the reaction into regions is illustrated in the compound-nucleus picture of nuclear reactions. The probability that a proton will be emitted from the N^{13} compound nucleus is given by

$$\Gamma_p = \frac{\hbar}{\tau} \sim P_\ell \frac{\hbar}{T},$$

where P_ℓ is the probability of the proton's leaving the nuclear surface and T is the average time for the compound nucleus to rearrange itself to emit the proton.[56] Now, P_ℓ is given by

$$P_\ell = \frac{4k}{K} v_\ell ,$$

where k is the wave number of the outgoing particle and K is the wave number within the nucleus. The term 4k/K comes from the reflection at the nuclear surface resulting from the abrupt change in wave length, and the factor v/ℓ indicates the effect of the Coulomb and centrifugal barriers. Accordingly we may write

$$\Gamma_p = (2k\, R v_\ell)\ \gamma_p ,$$

where R is the nuclear radius.[56] The first term represents the dependence upon conditions "outside" the nucleus and γ_p, the "reduced width," gives the dependence upon conditions within the nucleus. For an $\ell = 0$ outgoing proton we have

$$\Gamma_p \sim \sqrt{E}\ G\ \gamma_p ,$$

where G is the Gamow factor for penetration of the Coulomb barrier. Referring to Fig. 15, we see the experimental excitation function obtained for 15.1-Mev gamma rays compared with the energy dependence expected for an $\ell = 0$ outgoing proton, normalized so that the area under the curve is equal to the area under the second "point" (indicated by solid

horizontal line) above threshold. The curve for $\ell = 1$ outgoing protons did not even roughly approximate the data and hence was not drawn. We also note that the cross section drops above ~20 Mev, which may be accounted for by the fact that this is the threshold for the reactions $C^{12}(p, n)N^{12}$ and $C^{12}(p, pn)C^{11}$.

The fact that the energy dependence near threshold is consistent with $\ell = 0$ outgoing protons is in agreement with the measurements by Kavanagh,[14] who finds that the yield of 15.1-Mev photons in the reaction $B^{11}(d, n)C^{12*}$ varies as $\sqrt{E_n}$, as expected from $\ell = 0$ outgoing neutrons. In addition, Kavanagh found two resonances, presumably from the formation of compound states of C^{13}. The energy resolution obtainable in the $C^{12}(p, p')C^{12*}$ excitation function would not permit seeing comparable resonances from the formation of excited states of the N^{13} compound nucleus.

Figure 16 shows the excitation function from threshold to 340 Mev. The yield to 30 Mev was measured at 80° to the beam direction, and the yield above this energy was measured at 90°. These data are combined, as the yield is not expected to change significantly in this angular range. The absolute cross sections from the synchrocyclotron data (60 to 340 Mev) are subject to more uncertainty, as the beam current was determined by the thermocouple monitor (see Section II-A). The indicated errors include the error to be expected from this monitoring system.

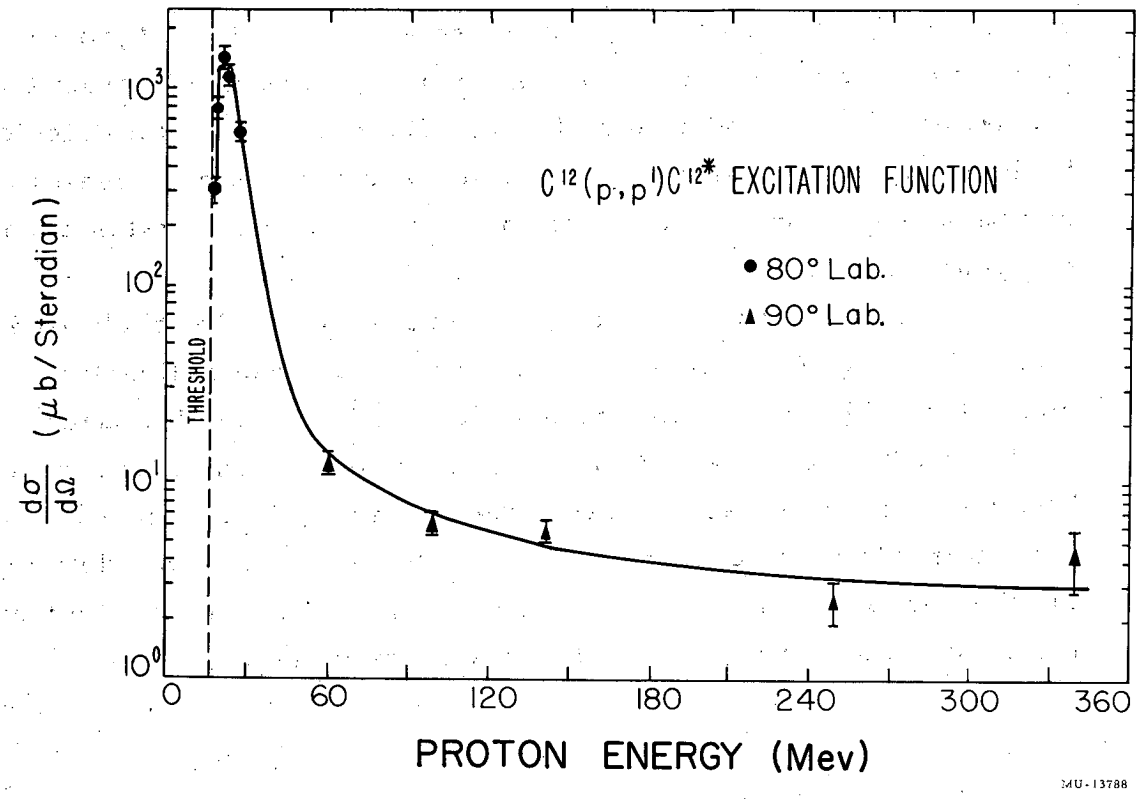

Fig. 16. Experimental excitation function for $C^{12}(p, p')C^{12*}$ 15.1 from threshold to 340 Mev.

C. Excitation by 90-Mev Neutrons

In connection with the problem of determining the reaction mechanism for higher proton energies, it was suggested that excitation might be occurring through the Coulomb field. In order to test this hypothesis it was decided to see if the excited level could be produced by inelastic neutron scattering. It was decided to use a NaI(Tl) crystal 3 in. in diameter by 3 in. long rather than the pair spectrometer because of its higher efficiency and greater mobility.

The neutron beam was produced by stripping the 180-Mev deuteron beam in a Be target.[58] The neutron flux was monitored with a bismuth fission chamber.[60] The NaI(Tl) crystal was viewed with a DuMont K1197 photomultiplier tube and the assembly was placed in a lead-brick structure that provided 4 in. of Pb on all sides. This was in turn covered with cadmium and paraffin to reduce the counting rate due to neutron background.

The energy calibration of the crystal was accomplished by using the 0.51- and 1.28-Mev gamma rays from a Na^{22} source in addition to the 4.43-Mev gamma ray from the first excited state of C^{12} produced by a PoBe source. In order to use the crystal over such an extreme energy range (0.51 to 15.1 Mev) the pulses were passed through an attenuator box, and this was used to change the effective gain of the system.

A series of target-in and target-out runs taken at several settings of the attenuator indicated that the 15.1-Mev level was being produced by the inelastic scattering of 90-Mev neutrons from the C^{12} target. This then served to indicate that the energy level was not being excited through the Coulomb field in the proton bombardment of C^{12}.

D. Alpha and Deuteron Bombardments

The conservation of isotopic spin in nuclear reactions requires that the states formed in reactions involving only alphas and deuterons have the same isotopic spin as the ground state of the bombarded nuclei.[61,62] This would prohibit the production of T = I states in the inelastic scattering of alphas and deuterons from C^{12}. The degree of inhibition of these reactions depends upon the purity of compound system as well as that of the initial and final states. Therefore it was decided to measure the yield of 15.1-Mev gamma rays in these forbidden reactions, and to make a comparison with the yield obtained in nonforbidden reactions.

The 184-inch synchrocyclotron was used to provide deuterons and alphas of sufficient energy to excite the 15.1-Mev level by inelastic scattering. A NaI crystal 3 in. in diameter by 3 in. long was used to detect the photons emitted at 90° to the internal beam. The crystal was placed outside the 20-foot-thick concrete wall and was shielded with 4 in. of Pb that was in turn covered with Cd sheet. This proved to give adequate neutron shielding, as the concrete wall had thermalized the emerging neutrons. The target was mounted in the thermocouple-monitor holder, but the usable beam intensities were so low that it did not operate. In fact, the beam had to be dropped below the level at which the ionization chambers within the shielding provided a useful monitor for the operators. To circumvent this difficulty, a counting-rate meter was used to monitor the rate at which pulses greater than $\sim$0.5 Mev were produced in the crystal. Outputs from this monitor were connected to a Leeds and Northrup Speedomax Recorder and to a meter installed in the control room. The 184-inch synchrocyclotron produces a burst of beam about 60 times per second. The width of the beam pulse depends upon the target radius but is of the order of 100 microseconds. The beam level was adjusted so that the counting-rate monitor indicated an average counting rate of 2 to 3 counts per beam pulse. Since the resolving time of the pulse-height analyzer was $\sim$10 μsec, this setting was more than adequate to insure that there would be no difficulties from dead time and pile-up in the measuring of gamma rays of $\sim$4 and 15 Mev.

To insure the production of 15-Mev gamma rays during the preliminary runs while the necessary instrumentation was being tested, a thick carbon target was bombarded with ~30-Mev protons. When it became apparent that it would be impossible to measure the internal beam current, it was decided to compare the yield of 15.1-Mev gammas with the yield of 4.43-Mev gammas in each reaction. The 4.43-Mev gamma ray results from the excitation of the first excited level in C^{12}, so that its yield gives an indication of the probability of an inelastic collision in the various bombardments. Also, since it is a T = 0 level there will be no inhibition of its yield from isotopic spin selection rules. The pulse-height distribution obtained from the proton bombardment of carbon is shown in Fig. 17, and the yield of 15.1-Mev gammas was 0.091 ± 0.009 of the yield of 4.43-Mev gammas.

Because the parameters for synchrocyclotron operation are essentially the same whether it is accelerating alphas or deuterons, an alpha beam has a large deuteron contamination if the accelerator contains residual deuterium from a recent deuteron bombardment. Circumstances made it necessary to examine the alpha-particle reactions shortly after a deuteron bombardment, and hence it was necessary to see if the deuteron contamination could be reduced.

In a fixed-frequency cyclotron deuterons and alphas are readily separated, as the slightly differing e/m ratios require different settings of the magnetic field. In the synchrocyclotron, the alphas should be captured into a stable "bunch" at a somewhat higher frequency than the deuterons. To use this effect to separate the alphas and deuterons, the various parameters were adjusted to obtain the maximum beam intensity and then the arc timing was adjusted to cause the arc to strike early, i.e., at a higher frequency. By adjustment of the arc timing only, the beam was reduced to the proper intensity as indicated by the counting-rate monitor (approximately 1/60 of full intensity). The spectrum of gamma rays obtained by bombarding a Be target showed the 4.43-Mev gamma ray originating from the decay of the first excited state of C^{12} produced in the reaction $Be^{9}(\alpha, n)C^{12*}$. To determine the effect a contamination of deuterons would have, the arc timing was

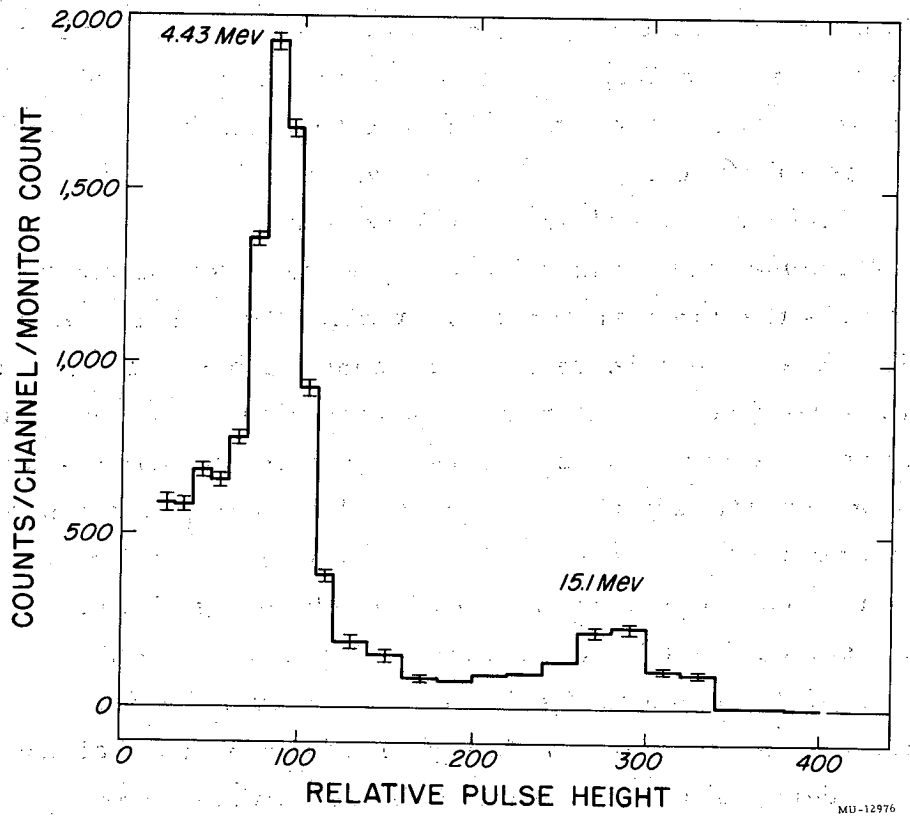

Fig. 17. NaI(Tl) pulse-height distribution from bombardment of a thick carbon target by 30-Mev protons.

adjusted until the same counting rate was obtained on the low-frequency side of the maximum setting. The spectrum did not indicate a 4.43- Mev gamma ray, showing that the intensity of alphas had been reduced below a measurable level. There were, however, two gamma rays of ~2 and 6 Mev present in the spectrum, and a careful search was made for their presence in the gamma-ray spectrum when the arc timing was returned to the previous setting. That these gamma rays could not be detected was taken to be an indication that the variation of arc timing had produced a beam of alphas reasonably free of deuteron contamination.

The gamma spectra obtained from bombarding thick targets of Be and C with 175-Mev alphas were obtained. The pulse-height distribution obtained in the bombardment of C is shown in Fig. 18. In the $Be^{9}(\alpha, n)C^{12*}$ reaction the yield of 15.1-Mev gammas was $1.25 \pm 0.22 \times 10^{-2}$ of the yield of 4.43-Mev gammas. In the inelastic scattering of 175-Mev alphas it appears that there may be a small yield of 15.1-Mev gammas superimposed on a continuum of higher-energy gamma rays. This yield is smaller than 2.7×10^{-3} the yield of 4.43-Mev gammas. After completion of the alpha runs the synchrocyclotron was changed to deuterons and the gamma-ray spectrum produced during the bombardment of a thick C target with 185-Mev deuterons was measured. Here there was no trace of a peak at 15.1 Mev, but uncertainty in yield due to the presence of a continuum of gamma rays permits the placing of an upper limit of 2×10^{-3} on the intensity of 15.1-Mev gammas relative to the intensity of 4.43-Mev gammas.

Later it was possible to measure the gamma spectrum produced by the inelastic scattering of 48-Mev alphas from carbon at the Crocker Laboratory 60-inch cyclotron. The experimental setup is shown in Fig. 19. The NaI(Tl) crystal viewed the thin target through a thin window on the side of the scattering chamber. A newly constructed shield was used that provided a minimum of 4 in. of Pb around the crystal-photomultiplier assembly. The Pb was enclosed in a layer of boron carbide for neutron shielding. In order to moderate the neutron flux so that it could be captured in the boron, the entire shield assembly was surrounded with blocks containing a mixture of boric acid power and paraffin. This

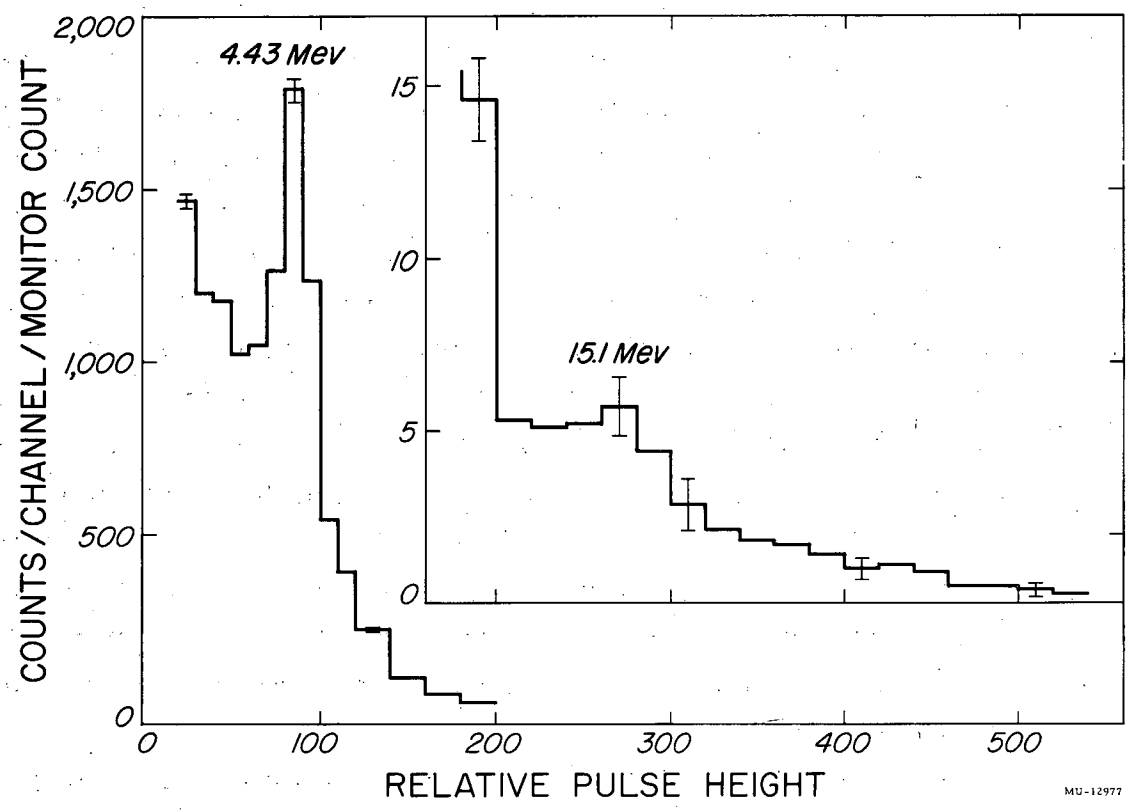

Fig. 18. NaI(Tl) pulse-height distribution from bombardment of a thick carbon target by 175-Mev alpha particles.

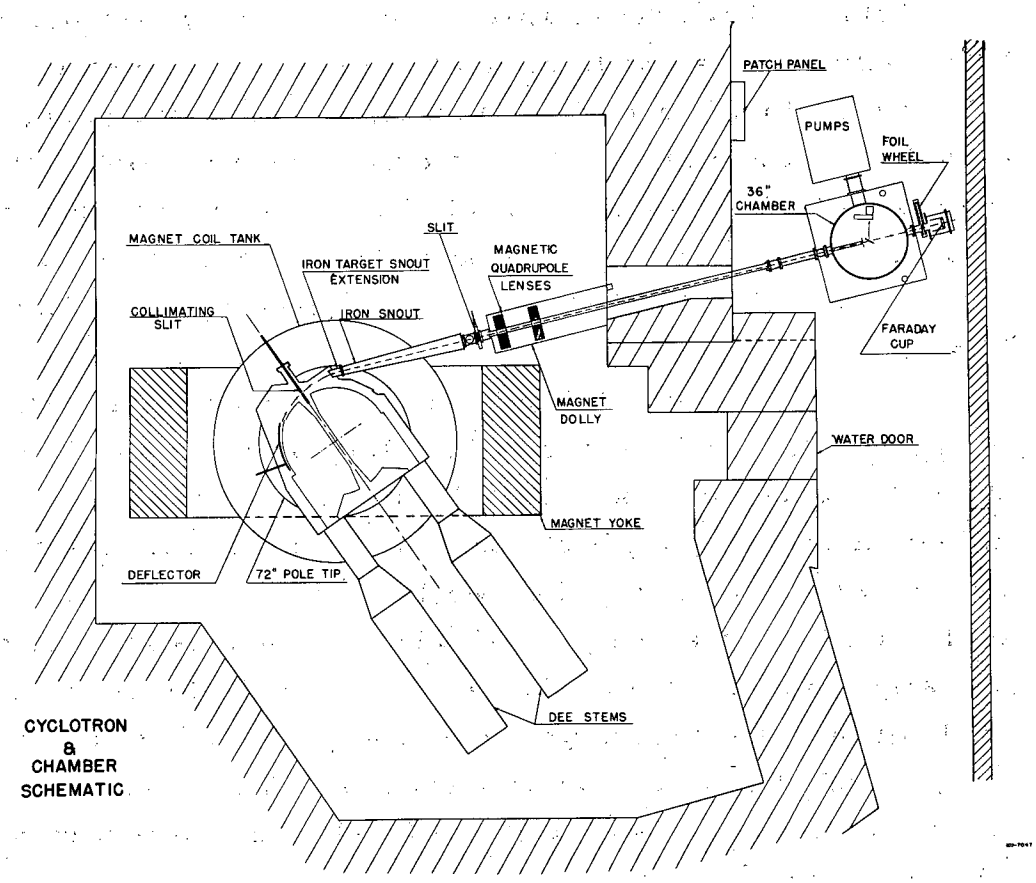

Fig. 19. Experimental arrangement at the 60-inch cyclotron. The NaI(Tl) crystal viewed the thin target through a thin window on the scattering chamber.

shielding arrangement reduced the background from the alpha beam to such an extent that the main background came from cosmic rays. The pulse-height distribution obtained in this run is shown in Fig. 20. There is no indication of any yield of 15.1-Mev gammas, and the absence of the gamma-ray continuum observed in the higher-energy bombardments permits placing an upper limit of 2×10^{-5} on the yield of 15.1-Mev gammas relative to the yield of 4.43-Mev gammas.

Table II shows the relative yields measured in various reactions. It is easily seen that the forbidden reactions give a lower ratio of yields than do the allowed reactions. Actually, in the higher-energy reactions there is the possibility that the outgoing deuteron or alpha will break up and permit the formation of a T = I state. That such a phenomenon could be occurring is indicated by the possible weak appearance of a 15.1-Mev gamma ray in the 175-Mev $C^{12}(\alpha, \alpha')C^{12*}$ data but not in the 48-Mev data (Fig. 18 and 20.)

The ratio obtained in the $Be^{9}(\alpha, n)C^{12*}$ reaction is quite different from the ratios obtained in the other allowed reactions. Some inhibition of the formation might be expected if Be^{9} were regarded as made up of two alphas and a loosely bound neutron, since merely replacing the neutron with the incoming alpha would not form a T = I state. Rasmussen et al. have found that the yield of $\sim$15-Mev gamma rays from a thick Be target with 21.7-Mev alphas was $\sim$6% the yield obtained from the bombardment of a thick target or B_4C with 10.8-Mev deuterons.[9] Unfortunately the ratio of gamma-ray intensities is not known for either of these experiments, so that it is difficult to compare them with the other reactions.

Rasmussen et al. were interested in determining the yield of 15.1-Mev gammas in the forbidden $N^{14}(d, \alpha)C^{12*}$ reaction. A 1-inch-thick NaI(Tl) crystal was used to detect the gamma rays. With a thick Melmac 404 ($N_6C_3H_6$) target they "obtained a small number of counts corresponding to γ radiation of $\geq$ 12.5 Mev." A photograph of an oscilloscope screen "indicated that this was probably the same γ ray observed with the boron target. Comparison of integral counting from the Melmac and B_4C targets, after subtraction of background, gave an intensity ratio of $\sim$0.03."

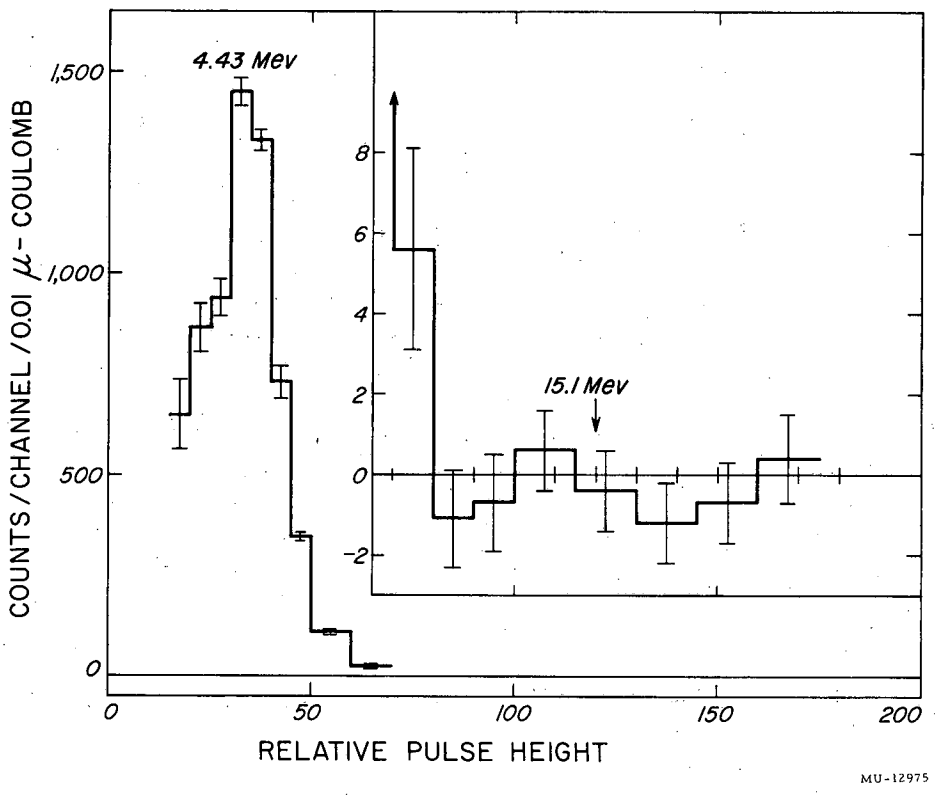

Fig. 20. NaI(Tl) pulse-height distribution from bombardment of a thin carbon target by 48-Mev alpha particles.

Table II

Relative yields of 15.1- and 4.43-Mev gamma rays in various reactions

	Reaction	Conditions	$I_{15.1}/I_{4.43}$	Notes
1.	$C^{12}(p, p')C^{12*}$	~30 Mev, thick target, 90°	0.091 ± 0.009	
2.	$C^{12}(p, p')C^{12*}$	30 Mev, thin target	~0.13	(a)
3.	$B^{10}(He^3, p)C^{12*}$	2 Mev, thin target	0.12 ± 0.007	(b)
4.	$Be^9(\alpha, n)C^{12*}$	175 Mev, thick target, 90°	$(1.25 \pm 0.22) \times 10^{-2}$	
5.	$C^{12}(d, d')C^{12*}$	85 Mev, thick target, 90°	$\leq 2 \times 10^{-3}$	(c)
6.	$C^{12}(\alpha, \alpha')C^{12*}$	175 Mev, thick target, 90°	$\leq 2.7 \times 10^{-3}$	(c)
7.	$C^{12}(\alpha, \alpha')C^{12*}$	48 Mev, thin target, 90°	$\leq 2 \times 10^{-5}$	(d)

(a) Assuming isotropy of 15.1-Mev radiation and comparing with cross section for 4.43-Mev level determined by Hecht.[51]

(b) From data of Almqvist, Bromley, Gove, and Litherland.[66]

(c) No discernible 15.1-Mev peak. Ratio is obtained from a continuum of higher-energy gamma rays.

(d) No discernible 15.1-Mev peak and no continuum of high-energy gamma rays.

[illegible] would expect to find [illegible] elastic scattering data, but there is no real basis for comparison, since the yield relative to the 4.43-Mev gamma ray is not known.

The results of these experiments are discussed further in Section IV.

E. Branching-Ratio Measurement for Radiative Decay

The 15-Mev level in C^{12} can decay through the emission of an α particle or through the emission of electromagnetic radiation. The observed 15-Mev gamma ray represents an electromagnetic transition from the 15.09-Mev level to the ground state. In addition to the ground-state transition there also are transitions to any one of the lower-lying excited states. In particular, one would expect to find a gamma ray of energy $E_\gamma = 15.1 - 4.43 = 10.67$ Mev corresponding to a transition to the first excited state. The first excited state is 2^+,[4] and if we identify the 15-Mev level as the analogue of the ground states of B^{12} and N^{12}, it is 1^+.[14,63]

Both transitions, then, would be expected to be magnetic dipole (M1), and on the basis of a single-particle transition probability[64] the relative intensities would be given approximately by

$$\frac{I_1}{I_0} \sim \left(\frac{E_1}{E_0}\right)^3 = \left(\frac{10.7}{15.1}\right)^3 = 0.36.$$

Examination of the earlier photon spectrum did not indicate the presence of a 10.7-Mev gamma ray. Therefore it was decided to remeasure the spectrum in an effort to determine the relative transition rates to the ground and first excited states.

Previous experience had indicated that the resolving power of the NaI(Tl) crystal was insufficient to detect the 10.7-Mev gamma in the presence of the 15.1-Mev gamma ray. It was decided to use the pair spectrometer described in Sect. II-A at the linear accelerator so that the excitation function could be continued to lower proton energies during the same run. A diagram of the experimental setup is shown in Fig. 21.

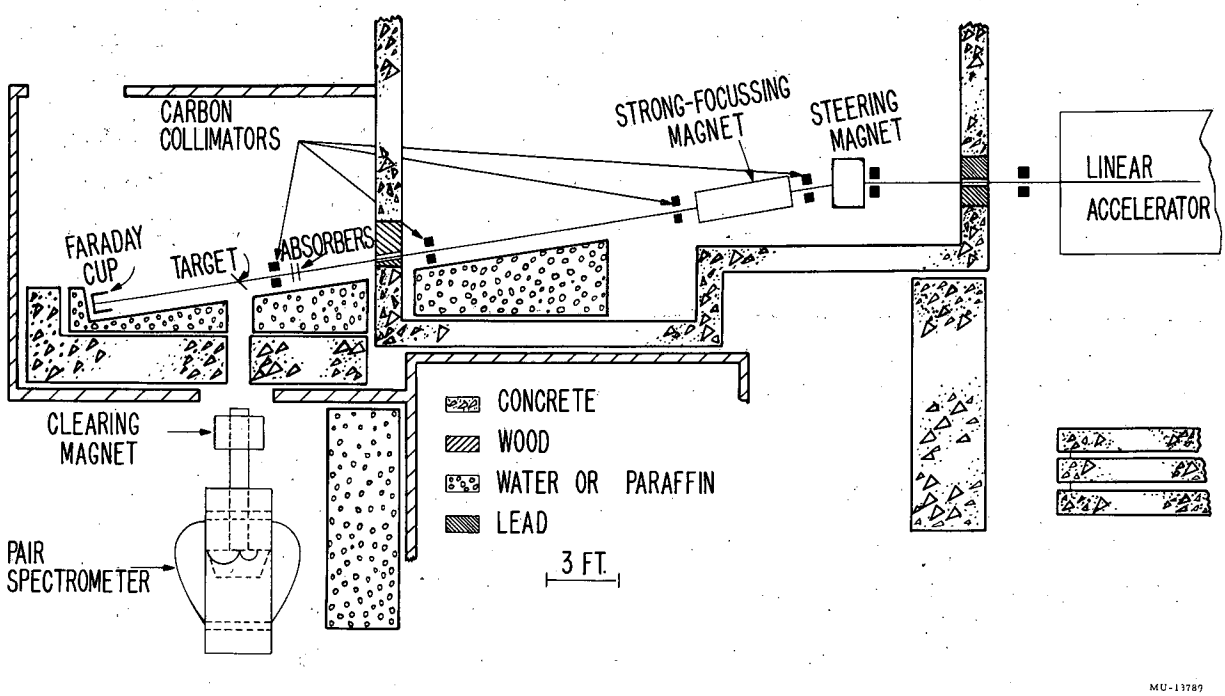

Fig. 21. Experimental arrangement at the 31-Mev proton linear accelerator.

The physical size of the 20-ton pair-spectrometer magnet made it necessary to place the spectrometer outside the linear accelerator building and to erect a temporary canvas shelter. This further required that the 31-Mev proton beam be brought out 40 feet beyond the end of the linear accelerator tank. The beam was focused on the carbon target by means of a set of strong-focusing quadrupole magnets.

Contrary to our previous experience in using the pair spectrometer at the 184-inch synchrocyclotron, a considerable background counting rate was found to be due to a flux of neutrons. This necessitated a great deal of effort to shield the spectrometer and to reduce the number of neutrons produced by the beam. It was found that a considerable fraction of the neutrons was being produced in the brass vacuum pipe, and this source was reduced, to a very large extent, by placing carbon collimators at regular intervals along the beam path. A new carbon-lined Faraday cup was built to reduce the neutron flux created when the beam was stopped. Additional shielding--consisting of a 2-foot-thick concrete wall, a tank of boric-acid-loaded water, and quantities of paraffin, boric acid powder, and cadmium--succeeded in reducing the background counting rate to a negligible amount.

The thickness of the carbon target was chosen so that the energy of the protons traversing the target was reduced below the threshold for producing the 15.1-Mev level. This procedure yielded the maximum photon intensity per incident proton flux. This was of some importance because the beam was run at maximum intensity at all times and the counting rates with the thin converter necessary for energy resolution were low.

In order to be able to detect the transition to the first excited state at all, it was necessary to adjust the field so that the 10.7-Mev gamma ray appeared at the center of the spectrometer range. At this field setting the 15.1-Mev gamma ray occurs in one of the highest channels at a reduced efficiency. Hence the yields of both the 10.7- and 15.1-Mev gamma rays were measured simultaneously so that one need know only the relative efficiency of the spectrometer for these gamma rays to determine their relative intensities. The efficiency calculations were

checked experimentally by changing the field so that the 15.1-Mev gamma ray appeared at the center of the spectrometer range. Close agreement was found between the observed yields and those expected from the efficiency calculations.

The spectrum of photons measured at 80° with respect to the 31-Mev proton beam is shown in Fig. 22. The spectrum shows the presence of a gamma ray of 12.8 ± 0.2 Mev in addition to the 15.1- and 10.7-Mev gamma rays. This gamma ray can be identified as the ground-state transition from the 12.76-Mev level in C^{12}.[4,14,18] The intensity of this gamma ray relative to the 10.76-Mev gamma is

$$\frac{I_{12.8}}{I_{10.7}} = 0.95 .$$

The ratio of intensities of the 10.7- and 15.1-Mev gamma rays under the conditions of observation is

$$\frac{I_{10.7}}{I_{15.1}} = 0.095 \pm 0.014 .$$

The relative intensities of these gamma rays were measured in two separate runs and the results of these runs were in agreement within the errors associated with the measurements. Only the data from the second run have been used, because the background was considerably reduced and the statistical errors are accordingly smaller.

The measured relative intensities of 10.7- and 15.1-Mev gamma rays give the relative transition probabilities only if the angular distributions for both gamma rays are the same. It was hoped that the angular dependence of the photon yield would be decreased by the spread in the proton energies in the target, but subsequent measurements by Almqvist, Bromley, Gove, and Litherland indicate a branching ratio of $2.4 \pm 1\%$.[18] In their experiment the 15.1-Mev excited state was produced in the $B^{10}(He^3, p)C^{12*}$ reaction. For the branching-ratio measurement they used two NaI(Tl) crystals, 5 in. in diameter by 4 in. thick, in coincidence. The 10.7-Mev gamma ray was detected by observing the spectrum

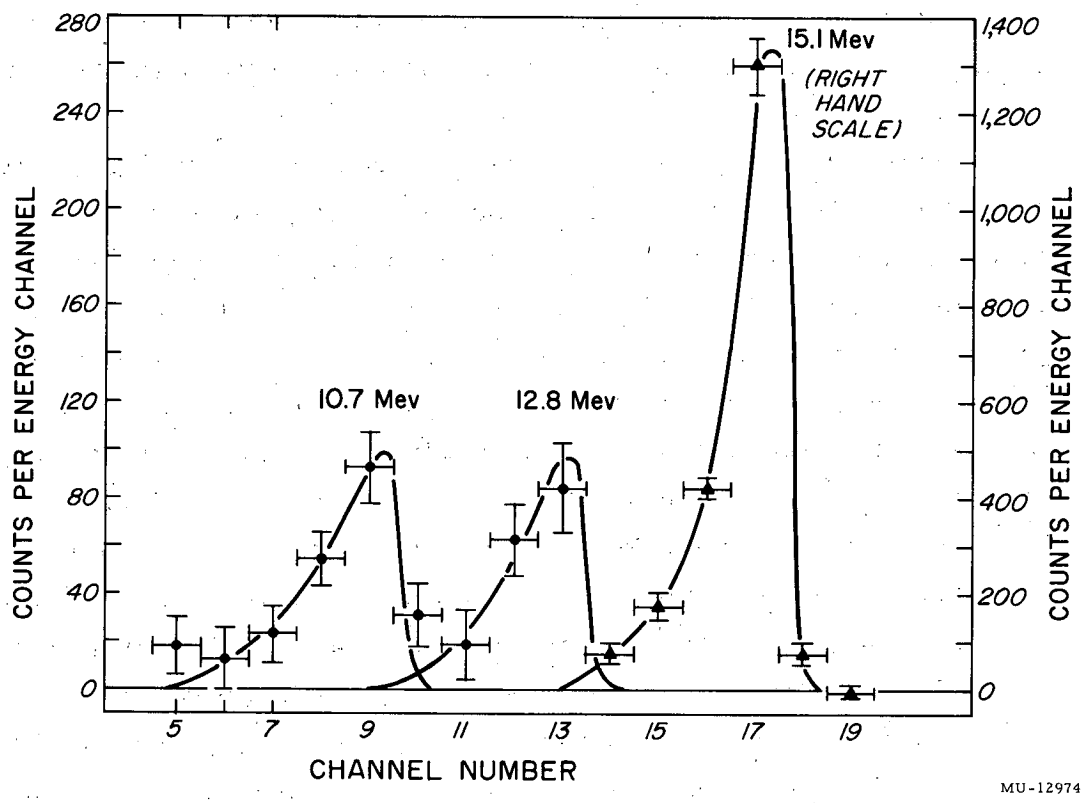

Fig. 22. Photon spectrum from bombardment of carbon target by 31-Mev protons.

in one crystal in coincidence with the 4.43-Mev gamma ray detected in the other. The crystals were placed close to the target so that each subtended a cone of about 40° half angle, thus tending to smear out any angular effects. Several measurements were made at different angles and each gave the same result. Their chief source of error arises from the uncertainty in subtracting from the coincidence spectra the contribution of the 11.7-Mev gamma ray resulting from the transition from the 16.1-Mev level in C^{12} to the first excited state. However, even if they omit this correction the branching ratio increases only to 3.8%.

Reference to the energy-level diagram of C^{12} in Fig. 1 indicates a number of levels whose excitation energy is greater than 16 Mev and that are known to decay via gamma transitions to the ground and first excited states of C^{12}. However, each of these states is known to decay primarily through particle decay.[4] In none of the various bombardments have we been able to detect a gamma ray of energy greater than 15.1-Mev. A particularly careful search was made during the run with the pair spectrometer at the linear accelerator for gamma rays corresponding to the higher excited states, but with no success. The resolution of the spectrometer is sufficient to separate clearly gamma rays of 10.7, 11.7, and 12.8 Mev, and no indication was found of an 11.7-Mev gamma ray.

From the analysis of the NaI(Tl) pulse-height distribution resulting from the observation of photons scattered at 120° by carbon, Fuller and Hayward place an upper limit on the intensity of gamma rays of $\sim$11 Mev as 10% the intensity of the 15.1 Mev gamma rays.[65] This limit presumably includes whatever contribution the 11.7- and 12.8-Mev gamma rays may make.

The differing measurements of the relative intensities of the 10.7- and 15.1-Mev gamma rays presumably indicate that the angular distribution is not the same for both gamma rays. The 15.1-Mev level is 1^{+} so that the transition to the 0^{+} ground state is M1. The transition to the 2^{+} first excited state is also M1, assuming pure multipole emission, but we must admit the possibility of the admixture of E2 radiation to the 2^{+} level. The angular distribution of both gamma rays is of the form

$1 + a_2 P_2 (\cos \theta)$ no matter what the mixture of the radiations,[66,67] and Almqvist has shown that the ratio of the a_2 coefficients is determined by the multipole mixture of the transition to the first excited state.[68]

To estimate the amount of mixed radiation present it is necessary to make some assumption concerning the nuclear forces. We may first consider a single-particle configuration, that is, one nucleon outside a closed shell subject to an ordinary potential V(r) due to the remaining nucleons. In this case Moszkowski[64] has shown

$$\frac{T(M1)}{T(E2)} = \frac{2.8 \times 10^{13} E_\gamma^{\ 3}}{1.6 \times 10^{8} A^{4/3} E_\gamma^{\ 5}} = 56 .$$

For the j-j coupling model according to which the nuclear wave functions are constructed from several independent single-particle wave functions,[69,70,71] Rose has shown[72] that a rough estimate of relative intensities is given by

$$\frac{T(M1)}{T(E2)} \sim \frac{(2L+3)^2}{(kR)^4} \left(\frac{\hbar k}{M_p C}\right)^2 \sim \left[\frac{25(2L+3)}{A^{2/3} E_\gamma}\right]^2 \sim 5 .$$

Because of the large difference in these estimates of the amount of mixing, it is desirable to see what empirical data exist. A survey of the radiative transition in light nuclei ($A \leq 20$) has been made by Wilkinson.[73] For each transition Wilkinson has calculated M^2, which is defined as the actual radiative width Γ_γ divided by the single-particle shell-model estimate (Weisskopf unit), $\Gamma_{\gamma W}$, appropriate to that type (multipole order and parity change) of transition. The data indicates that for E1 transitions the distribution of M^2 centers on $M^2 = 0.032$ and that a variation by a factor of seven in transition speed on either side of this value covers 85% of the transitions. The distribution for M1 transitions centers on $M^2 = 0.15$, with a variation of 20 on either side of the mean necessary to include 85% of the transitions. The number of E2 transitions known is small (only 8), so that it is rather difficult to draw general conclusions. If we average the values of M^2 for which the

radiative widths are well known, we find M^2 av = 1.5 for E2. As pointed out by Wilkinson, this enhancement of speed may be due to experimental bias in that only the strongest transitions can be seen.

We may now utilize these results to correct the single-particle-model estimate of the amount of admixture of E2 radiation present:

$$\frac{T(M1)_{ave.}}{T(E2)_{ave}} \sim \frac{0.15\ T(M1)}{1.5\ T(E2)} \sim 5.6.$$

This estimate agrees with the second calculation, but represents only a rough estimate because of the range of values of M^2 obtained for both M1 and E2 transitions.

IV. ISOTOPIC SPIN

Quantum-mechanically the conservation laws arise from the invariance of the Hamiltonian operator with respect to certain transformations of the frame of reference in which ψ is described. The dynamic variable T was introduced by Wigner[74] as a quantity that should be a constant of the motion, or "a good quantum number," with a charge-independent Hamiltonian. The choice of a charge-independent Hamiltonian is in accord with the empirical evidence from high-energy nucleon-nucleon scattering that the nuclear portion of the p-p interaction is the same as that of the n-p interaction.[75, 76] The symmetry of the purely nuclear parts of the n-n and p-p interactions is indicated by the close agreement in mass of the ground states of mirror nuclei after subtraction of electrostatic effects and the neutron-proton mass difference.[4, 12]

As the Coulomb interaction between protons constitutes a deviation from charge independence of nuclear forces, the application of an isotopic-spin formalism to the problem of nuclear structure is restricted to the light nuclei. The assumption of charge independence permits the prediction of relationships between the states of isobaric nuclei. The mirror nuclei, such as He^5-Li^5 and Be^7-Li^7, differ only in the exchange of a single neutron for a single proton, and hence, as regards the intranuclear forces, only in the replacement of some neutron-neutron bonds for proton-proton bonds. Examination of the level structure of the mirror nuclei[12] indicates a one-to-one correspondence of the excited states as regards spin, parity, and energy, after correction for the neutron-proton mass difference and the Coulomb energy. In a set of even isobars, such as Be^{10}, B^{10}, and C^{10}, the outer members (Be^{10}-C^{10}) differ only in the exchange of a neutron pair for a proton pair, and the level structures of the two nuclei correspond as in the case of the mirror nuclei. The center member (B^{10}), having substituted a n-p bond for n-n or p-p bonds, has states that are forbidden for the outer pair by the Pauli Exclusion Principle, in addition to the analogue states. Thus, the hypothesis of charge independence of nuclear forces predicts that every state of the asymmetric members will have an analogue in the symmetric one, but not vice versa.

In addition to predicting relationships between the stationary states of isobaric nuclei, the assumption of charge independence also leads to predictions concerning the dynamic properties of nuclear reactions. Adair[61] and Kroll and Foldy[62] have discussed the restrictions imposed on heavy-particle reactions when isotopic spin is conserved in nuclear reactions. In particular, in reactions involving the emission and absorption of particles with $T = 0$, such as deuterons and alpha particles, the initial and final states must have the same isotopic spin. The existence of selection rules for the emission and absorption of electric dipole radiation was first pointed out by Trainor,[77] and since then Radicati[78] and Gell-Mann and Telegdi[79] have shown that for any multipolarity of radiation, whether electric or magnetic, the selection rule is $\Delta T = 0, \pm 1$, with the limitation that the selection rule is $\Delta T = \pm 1$ for electric dipole transitions in self-conjugate nuclei, neglecting higher-order terms in the E1 operator. However, it has been shown by MacDonald that these higher-order terms are much less effective than the isotopic-spin impurity of states in producing violations of the isotopic-spin selection rules.[80]

Even under the conditions that the specifically nuclear portion of the internuclear interaction is charge-independent, isotopic spin cannot strictly be a good quantum number because of the existence of Coulomb forces. The effect of the Coulomb interaction is to mix states of different isotopic spin but of the same spin and parity. This mixing of states of differing isotopic spin results in a lessening of the effectiveness of the isotopic-spin selection rules. Thus by examining the validity of the isotopic-spin selection rules it is possible to determine the extent to which mixing of states is occurring, and to compare this with the amount of mixing attributable to the Coulomb interaction.

Unfortunately, as pointed out by Adair,[61] the amount of isotopic spin impurity is difficult to determine from reactions involving $T = 0$ particles or from radiative transitions as the transition probabilities are proportional to the squares of the isotopic-spin mixing coefficients.[61] Thus, a reaction leading to a state consisting of a mixture of 10% of a wave function the reaction to which is allowed and 90% of a wave function the transition to which is forbidden will result in a yield of the order of only

1% of a completely allowed reaction. Barker and Mann indicate that the relative number of protons and neutrons emitted from an excited state of a self-conjugate nucleus produced via E1 absorption can give a sensitive test of mixing, since the mixing coefficients enter linearly into the transition probabilities.[81] The giant resonances are generally ascribed to E1 absorption, but all other multipoles can produce both T = 0 and T = 1 excited states and cause different proton and neutron emissions.

An extensive investigation of the validity of isotopic-spin selection rules has been conducted by Wilkinson with various collaborators.[82-91] For the most part the experiments have been concerned with the selection rule $\Delta T = \pm 1$ for E1 transitions in self-conjugate nuclei. To obtain a measure of the impurity of excited states it is necessary to compare the measured widths for forbidden transitions with the expected widths for nonforbidden transitions. In order to make this comparison, Wilkinson has compiled the known radiative widths for various multipole transitions occurring in the light nuclei.[73] It is to be noted that the selection rule involving self-conjugate nuclei does not test charge independence, but only charge symmetry, i.e., that n-n = p-p. The T = 1 impurities expected for the T = 0 ground states of light nuclei as a result of Coulomb mixing have been calculated by Radicati[91] and MacDonald.[92] It is expected that the impurity of the higher excited states should be greater because of the closer proximity of states of the same spin and parity but differing isotopic spin.

The mixing of T = 0 in the 15.11-Mev state would result in a relaxation of the selection rule prohibiting the production of the state by $C^{12}(\alpha,\alpha')C^{12*}$, $C^{12}(d,d')C^{12*}$, and $N^{14}(d,\alpha)C^{12*}$ as well the decay of the state through the emission of an alpha particle. To the extent that the production of this state by incoming alphas and deuterons proceeds through an intermediate compound nucleus, the strength of the reaction depends upon the impurity of the compound system as well as upon the impurity of the initial and final states. The probability of alpha emission to the first excited state of Be^8 is also governed by the impurity of initial and final states. However, the impurity of the low-lying levels

should be very closely the same as that of the ground state, and for Be^8 the amount of $T = 1$ admixture in the $T = 0$ ground state has been calculated[92] to be

$$a_0^2(1) \simeq 4.4 \times 10^{-4}.$$

It is therefore desirable to use information in the probability of α emission to estimate the isotopic spin impurity and then compare with the results obtained from reaction data.

From measurements of Γ_t and Γ_{γ_0}, Fuller and Hayward give $18.65 \leq \Gamma_\alpha \leq 24.5 \pm 8.2$ ev.[21] The spread in Γ_α comes from ascribing a radiative-transition probability to the first excited state of C^{12} of 0 to 10% that of the ground-state transition (see Sect. III-3). We may estimate the amount of mixing by comparing the observed α width to that expected for an uninhibited transition. This may be done by comparing the "reduced widths" that result when one removes the dependence of the transition probability upon the probability of penetrating the Coulomb and centrifugal barrier.

We may first write

$$\Gamma_\alpha = 2 k R P_\ell \gamma_\alpha$$

where k is the wave number of the He^4-Be^8 pair; P_ℓ is the penetrability, and γ_α is the reduced width for alpha-particle emission.[93] The penetrability is given by

$$P_\ell = \frac{1}{F_\ell^2(R) + G_\ell^2(R)}$$

where $F_\ell(R)$ and $G_\ell(R)$ are the "regular" and "irregular" solutions of the radial wave equation.[94, 95] If the 15.11-Mev level is 1^+, particle decay must occur through d-wave alphas to the 2.90-Mev 2^+ first excited state of Be^8. For R we choose $R = 1.40 (A_1^{1/3} + A_2^{1/3}) \times 10^{-13}$ cm $= 5.0 \times 10^{-13}$ cm, in accord with the results of α scattering on carbon and oxygen,[96] and obtain

$$42 \text{ ev} \leq \gamma_a \leq 55.5 \text{ ev.}$$

The amount of isotopic-spin impurity can now be obtained from a comparison of γ_a observed with that expected for an uninhibited transition. For a single-particle excitation the reduced width is given approximately[97] by

$$\gamma_a \simeq \gamma_{aS} = \frac{\hbar^2}{\mu R^2} = 3.6 \times 10^6 \text{ ev.}$$

If many particles are excited, then the reduced width may be expressed by

$$\gamma_a = \frac{3\hbar^2}{2\mu R^2} \sum_n C^2_{\lambda Sn} ,$$

where the $C_{\lambda Sn}$ give the strengths of the individual wave functions. The sum of $C^2_{\lambda Sn}$ will in general be much less than one, but setting it equal to one we obtain the "Wigner limit,"

$$\gamma_a \leq \gamma_{aW} = \frac{3\hbar^2}{2\mu R^2} = 5.4 \times 10^6 \text{ ev.}$$

Use of the Wigner limit permits one to place a lower limit on the intensity of the isotopic-spin impurity,

$$a_1^2(0) \geq \frac{\gamma_a}{\gamma_{aW}} = 7.9 \times 10^{-6} .$$

Observed α widths vary from the single-particle width to ~ 0.001 of that width,[94-96,98] so that one cannot with certainty do more than to establish a lower limit for the isotopic-spin impurity. However, the few large widths are probably due to a single-particle excitation where the alpha particle retains its identity in the compound nucleus. The very small widths are associated with transitions forbidden by isotopic-spin selection rules. Within a factor of ten we would expect an uninhibited transition to have $\gamma_a \simeq 0.01\ \gamma_{aS}$, giving

$$a_1^2(0) \simeq \frac{\gamma_a}{0.01\ \gamma_{aS}} = 1.4 \times 10^{-3} .$$

This may be compared with the theoretical figure of MacDonald for the ground state of C^{12}, namely $a_0^2 \simeq 1.9 \times 10^{-3}$.[92] It is of interest to note that the "intensity" of the isotopic-spin impurity for the 15.1-Mev level is the same as that of the ground state within an order of magnitude.

Further information on the mixing of isotopic spins is obtained from the experiments measuring the yield of the forbidden reactions. From Table II of Section III-D we can estimate that, within an order of magnitude, an allowed reaction would give a yield of 15.1-Mev gamma rays of approximately 5% the yield of 4.43-Mev gamma rays. With this estimate we may calculate an effective isotopic-spin impurity $a_{1\,\text{eff.}}^2(0)$, defining it as the ratio of the forbidden yield to the yield expected for an allowed reaction.[85] The quantity $a_{1\,\text{eff}}^2(0)$ is determined by the purity of the initial and final states and also by the way the nucleus is excited. The values of $a_{1\,\text{eff}}^2(0)$ are tabulated in Table III.

Table III

Effective isotopic spin impurities observed in various reactions

Reaction	$I_{15.1}/I_{4.43}$	$a_{1\,\text{eff}}^2(0)$[a]
5. $C^{12}(d,d')C^{12*}$	$< 2 \times 10^{-3}$	$< 4 \times 10^{-2}$
6. $C^{12}(\alpha,\alpha')C^{12*}$	$< 2.7 \times 10^{-3}$	$< 5.4 \times 10^{-2}$
7. $C^{12}(\alpha,\alpha')C^{12*}$	$< 2 \times 10^{-5}$	$< 4 \times 10^{-4}$

[a] Assuming $I_{15.1}/I_{4.43} = 0.05$ for an allowed transition.

The relative amplitude of the state of isotopic spin T' which the Coulomb forces mix with the state of isotopic spin T is given by

$$a_T(T') = \sum_{T'} \frac{H^C}{\Delta E} ,$$

where ΔE is the energy separation of the state T and those of T' of the same spin and parity that are being mixed by H^C, the Coulomb matrix element. It has often been assumed that $a_T(T')$ would be larger for highly excited states, since ΔE is smaller. This will be true only if the matrix elements connecting near-by states are as large as the matrix elements for more distant states. Actually it appears that the large matrix elements of the Coulomb interaction are those arising from excitation of the core.[88, 92, 99] In this case ΔE is also large, so that the contribution to a^2 is not large. The calculations by Barker of Coulomb matrix elements connected $T = 0$ and $T = 1$ states of C^{12} in L-S coupling show that matrix elements are smaller for states of the same configuration than for states of different configurations.[99] From this it can be seen that one should not expect highly excited states to necessarily have large isotopic-spin impurity.

According to a compound-nucleus picture of reactions of (d, d'), (α, α'), and (d, α) types, the intermediate nucleus can be excited in the region of overlapping levels. In this case it is the effective isotopic spin of the several excited states that governs the reaction rate. Wilkinson has suggested that the amount of mixing is a time-dependent phenomenon.[88] Upon formation the compound system has an isotopic spin the same as that of the initial system, but as time passes the Coulomb forces perturb this total state and cause the growth of other isotopic spin states. Thus the observed mixture of isotopic spin states depends upon the lifetime of the compound nucleus.

Vaughn has found good evidence in the inelastic scattering of 48-Mev alphas from C^{12} and Mg^{24} that this reaction proceeds via a direct interaction process.[100] The time required for such interactions is short, so that one would expect only a small amount of mixing. The N^{14}(d, α)C^{12*}

reaction presumably proceeds through the formation of the compound nucleus O^{16*}. In the thick-target experiments by Rasmussen et al., the compound nucleus would have excited states from 20 to 31 Mev.[9] For this excitation of O^{16}, Wilkinson's data would predict $a_{l_{eff}}^2(0) \leq 0.1$.[88]

The observation of $\sim$15-Mev gammas by Rasmussen et al. may be an indication that the intermediate system has a longer life in the $N^{14}(d,a)C^{12*}$ reaction than in the $C^{12}(a,a')C^{12*}$ reaction, even though the excitation energies are comparable in both reactions.

V. SUMMARY

It has been established that the 15-Mev gamma ray originally reported is the result of the radiative transition from the 15.1-Mev level in C^{12}. The inhibition of alpha decay and the inhibition of the production of this level by reactions forbidden by the isotopic-spin selection rules indicate that this level is T = 1. The excitation energy and the measurement of J = 1 indicate that this level is the analogue of the ground states of B^{12} and N^{12}. This identification permits the assignment of positive parity to the state.

The excitation function for the production of this state by the inelastic scattering of protons has been measured from threshold to 340 Mev. The variation in yield near threshold is shown to be consistent with that expected from the penetration of the Coulomb barrier by $\ell = 0$ outgoing protons. The variation in yield for higher-energy protons ($\sim$60 to 340 Mev) is in agreement with calculations based on assumption of excitation through the collision of the incoming proton with a nucleon within the entire volume of a spherical nucleus.

The radiative transition from the 15.1-Mev level to the first excited state of C^{12} has been detected. At 80° to the direction of the incident 31-Mev proton beam the branching ratio is 0.095 ± 0.014 with a thick carbon target. The branching ratio has been measured as 0.024 ± 0.01 by Almqvist, Bromley, Gove, and Litherland under conditions that would smear out any angular effects. These differing measurements presumably indicate that the angular distribution is not the same for both gamma rays.

Comparison of the reduced widths for alpha emission to that expected for an allowed transition indicates that the intensity of T = 0 mixture in the 15.1-Mev level is comparable to the intensity predicted for the ground state. This can be interpreted as meaning that the Coulomb matrix elements mixing near-by states are smaller than those mixing distant states.

Experiments comparing the yield of 15.1-Mev gamma rays in isotopic-spin forbidden and allowed reactions permit the calculation of effective isotopic-spin mixing coefficients. For the inelastic scattering of 48-Mev alpha particles from C^{12}, experimental conditions permitted

placing an upper limit on $a_{1_{eff}}^2(0)$ that is smaller than the value expected for a reaction proceeding through the O^{16*} compound nucleus. This indicates that the reaction probably proceeds through a direct-interaction process and that the lifetime of an intermediate system is too short to permit effective mixing of states of differing isotopic spin.

ACKNOWLEDGMENTS

I shall always be grateful to Professor Burton J. Moyer for his guidance, encouragement and patience. The many contributions of my colleagues, Harold Adelson, Dr. David Cohen, and Harlan Shaw, during various phases of the experiment are gratefully acknowledged.

I am indebted to Drs. Dennis H. Wilkinson, William MacDonald, and Warren Heckrotte for several stimulating discussions. Mr. Gilbert Mead and Mr. John Young were extremely helpful in the preparation of the program for IBM-650 Computer calculations.

The successful completion of an experiment at a laboratory as large as UCRL requires the teamwork of many variously talented people. It is unfortunately impossible to mention each person by name, but the contribution of each is none the less appreciated. I do want to thank the crews of the synchrocyclotron under Mr. James Vale, and of the linear accelerator under Mr. James Sirois, for their efficient and cooperative assistance.

This work was done under the auspices of the Atomic Energy Commission.

APPENDICES

1. Angle of Emission of Pairs

In the process of creating a pair of positive and negative electrons through the absorption of a γ ray, energy and momentum conservation are possible only if another particle is present (for instance, a nucleus). As we are dealing with a three-body system, there does not exist a unique angular relationship between the electron-positron pair and the direction of the incident photon. However, since the electric vector of the radiation has no component in the direction of the radiation, there are no electrons ejected directly forward. Also, as the mass of the electrons is so much smaller than that of a nucleus, the electron pair carries away most of the energy of the γ ray and thus the center of gravity of the pair should move almost collinearly with the photon.

The process of pair production is closely allied to bremsstrahlung, so that one may obtain the differential cross section for pair production from the Bethe-Heitler formula for bremsstrahlung.[101, 102] As a consequence of the use of the Born approximation the electron and positron are treated symmetrically, whereas the nucleus repels the positron and attracts the electron. This effect is greatest for small electron velocities (i.e., low-energy photons) and for high-Z material. The result is to decrease the probability for pair production when p^+ is small and increase it when p^- is small. Thus the positron is emitted with an average angle smaller than that of the electron. The angular distribution at low energies has been studied experimentally by Simons and Zuber,[103] Groshev and Frank,[104] and Groshev.[105] The results indicate that although the mean angle of emission for light elements agrees with the prediction of the Born approximation, for heavier elements they increase with atomic number, and the value for the positron is smaller than that for the electron.

A useful approximation to the angular distribution predicted by the Bethe-Heitler formula is given by Heitler.[102] The number of electrons (positrons) emitted between angles $\underline{\Phi}$ and $\underline{\Phi} + d\underline{\Phi}$ is given by

$$N(\underline{\Phi})\, d\underline{\Phi} \propto \frac{\underline{\Phi} d\underline{\Phi}}{(\underline{\Phi}_p^2 + \underline{\Phi}^2)^2},$$

where

$$\Phi_p = \frac{mc^2}{E} .$$

The angle at which maximum electron emission takes place is found by differentiation to be

$$\Phi_{max} = \frac{\Phi_p}{\sqrt{3}} ,$$

and the angle of bipartition, defined so that half the electrons are emitted within it and half outside it, is closely given by Φ_p.[23]

2. Multiple Scattering of Electrons

As an electron traverses the converter it undergoes a large number of collisions, most of which produce very small angular deflections. We wish to compute the probability that an electron emerges from the plate with a given angular deflection as a result of these successive collisions. From Rossi,[55] Sect. 2.16, we obtain the following formulas:

$$\Theta_S^2 = \left(\frac{E_S}{\beta C_p}\right)^2 \frac{1}{X_0} ,$$

and

$$\langle \Theta^2 \rangle_{av} = \Theta_S^2 \, x \text{ (for no energy loss)},$$

where

$\langle \Theta^2 \rangle_{av}$ = mean square angle of scattering,

X_0 = radiation length, $\frac{1}{X_0} = 4\alpha \frac{N}{A} Z^2 r_e^2 \ln \frac{183}{Z^{1/3}}$,

x = thickness in radiation lengths,

E_S = 21 Mev,

$\beta C_p = T$ = kinetic energy for relativistic particles.

The above formulae are derived with the assumption of Rutherford scattering by a point charge, with angular deviations limited by screening at small angles and by the finite size of the nucleus for large angles.

The converter thickness at which multiple scattering becomes more important than the natural angular spread of the electrons due to the pair-production process is independent of energy because both angles vary inversely with energy. To estimate the relative importance of the two processes we may compare $\phi_p = mec^2/E_\gamma$ to the rms scatter ng angle of an electron of energy $T = E_\gamma/2$;

$$\frac{\Theta_{rms}}{\phi_p} = \frac{\frac{21}{T}\sqrt{\frac{x}{X_0}}}{\frac{mc^2}{E_\gamma}} \cong 82\sqrt{\frac{x}{X_0}} ,$$

$$\Theta_{rms} = \phi_p \text{ for } x_c \simeq \frac{X_0}{82^2} \simeq 1.5 \times 10^{-4} X_0 .$$

Using $X_0 = 6.35\ g/cm^2$ for T_a we find $x_c = 9 \times 10^{-4}\ g/cm^2$, a thickness that is much smaller than the thinnest converter used in the experiment. The above conclusions are qualitatively in agreement with the observations of Kinsey and Bartholomew,[25] who began to notice the effects of multiple scattering with a gold converter of ~ 7 mg/cm^2 or $1.2 \times 10^{-3} X_0$. The converters used in the spectrometer were always much thicker than x_c so that multiple scattering is the dominant process determining the electron angular distribution.

The angular spread in the electrons affects the spectrometer in two ways:

(a) Scattering of the particles in a vertical direction causes them to miss the G-M tubes, thus reducing the efficiency of the spectrometer.

(b) Scattering of the particles in a horizontal direction causes the electrons to reach the plane of the G-M tubes with a smaller apparent radius of curvature because of the focusing properties of the 180° geometry.

Thus we find it convenient to consider the projection θ of the total deflection on a plane containing the original trajectory. For small angles we have

$$\langle \theta^2 \rangle_{ave} = \frac{1}{2} \langle \Theta \rangle^2_{ave} = \frac{1}{2} \Theta_S^2 x .$$

From Rossi, Sect. 2.17 (loc. cit.) we can obtain the distribution function for a beam of particles traversing a thickness x of material. Letting the y axis be the horizontal axis and the Z axis the vertical axis, we let $P(x, y, \theta_y)dy, d\theta_y$ be the number of particles at thickness x having a lateral displacement that falls within dy at y and traveling at an angle within $d\theta_y$ at θ_y. For small angular deflections and no energy loss, we have

$$P(x, y, \theta_y)\, dy\, d\theta_y = \frac{2\sqrt{3}}{\pi} \frac{1}{\Theta_S^2 y^2} \exp\left[-\frac{4}{\Theta_S} \left(\frac{\theta_y^2}{x} - \frac{3y\theta_y}{x^2} + \frac{3y^2}{x^3} \right) \right] .$$

We may neglect the lateral displacement in the foil, as the converters used are thin. By integrating P over y we obtain the function $Q(x, \theta_y)$ that represents the angular distribution:

$$Q(x, \theta_y) = \int_{-\infty}^{+\infty} P(x, y, \theta_y)\, dy = \frac{1}{\sqrt{\pi}} \frac{1}{\Theta_S x^{1/2}} \exp\left(-\frac{\theta_y^2}{\theta_S^2 x} \right) .$$

From considerations of symmetry we have

$$Q(x, \theta_Z) = \frac{1}{\sqrt{\pi}} \frac{1}{\Theta_S x^{1/2}} \exp\left(-\frac{\theta_Z^2}{\Theta_S^2 x} \right)$$

and

$$\int_{-\infty}^{+\infty} Q(x, \theta_y)\, d\theta_y = 1 .$$

3. Straggling of Electron Energy Due to Converter Thickness

Electrons produced within the converter lose energy by means of collisions with the atomic electrons, and by the emission of bremsstrahlung in the Coulomb field of the nucleus. The interaction of the incident electrons with the atomic electrons is characterized by the fact that the energy transferred to the atoms per collision is small. On the other hand, in the emission of radiation an electron may lose a large fraction of its energy in the form of a single high-energy photon. We would thus expect a small amount of straggling to be due to collision loss, whereas the straggling as a result of radiation should be large.

Actually, the straggling in energy loss due to collisions of a beam of electrons traversing a foil is increased by the fact that multiple scattering of the electrons causes a statistical variation in true path lengths. In addition, it is possible for an electron in a single collision with another electron to lose up to one-half of its energy.[106] Experimentally, we are concerned with the probable energy loss due to collisions in passing through a foil, which is given by[107]

$$\Delta E_C = 0{,}153\ \rho x \frac{Z}{A} \left[\ell n \frac{x}{x_0} + 19.45 \right] \text{Mev},$$

$$x_0 = 1 \text{ cm},$$

and the half width is given by

$$\Gamma_C = 0.61 \quad \rho x \frac{Z}{A} \beta^{-2} .$$

Table IV shows the probable energy loss due to collisions of an electron of $\beta = 1$ passing through the converters used in the spectrometer.

Table IV

Probable energy loss by electrons from collisions

x g/cm^2	ΔE_C (Mev)	Γ_C (Mev)	$\Gamma_C/\Delta E_C$
0.02974	2.41×10^{-2}	7.32×10^{-4}	3.04×10^{-62}
0.13968	1.27×10^{-1}	3.44×10^{-3}	2.71×10^{-62}

The resolution width for gamma rays due to collision loss is $2\Delta E_C$, since both electron and positron lose energy in traversing the converter. Because both particles lose energy independently, the half width for a given X is $\sqrt{2}\,\Gamma_C$. The line shape of the spectrometer due only to collision loss is shown in Fig. 6.

The problem of straggling of energy due to radiation loss has been treated by H. Bethe and W. Heitler,[101] J. Richards and L. Nordheim,[108] and L. Eyges.[109] The essential difference between the treatments of this problem by the various authors cited is in the use of different approximate expressions to represent the intensity-distribution curves in various electron-energy ranges. The results of Bethe and Heitler are in a convenient form for use, as only small changes in parameters permits the use of Pearson's Tables of the Incomplete Γ Functions.[110] The approximation used in this calculation is appropriate to electrons of energy greater than ~ 25 Mev, and it therefore overestimates the amount of straggling at energies of concern in this experiment.

From Heitler, Sect. 37,[102] we find that the probability that an electron still has an energy greater than e^{-y0} times the initial energy after traversing a sheet of material is given by

$$W(b\ell, y0) = \frac{\int_0^{y0} e^{-y}\, y^{b\ell-1}\, dy}{\int_0^{\infty} e^{-y}\, y^{b\ell-1}\, dy} = \frac{(b\ell-1,\ y^0)!}{\Gamma(b\ell)} ,$$

where

$(b\ell^{-1}, y0)!$ is the "Incomplete Γ-Function,"

$$b = a\ N\ \frac{Z^2\ r_0^2}{137},$$

N = number of atoms/gram,

ℓ = length in g/cm^2,

r_0=classical electron radius,

and "a" is a parameter that determines the shape of the formula approximating the intensity distribution curves. The parameter "a" varies only slightly in value; it is about 20 for Pb and 23 for H_2O. The converters used during this experiment were made of tantalum, and using a value of 20 for "a" we determine that $b = 0.206\ cm^2/g$. The thickest converter used in the experiment was $0.137\ g/cm^2$ ($b\ell = 2.8 \times 10^{-2}$), therefore we are interested in the straggling for foils with $b\ell < 3 \times 10^{-2}$. Using Pearson's tables,[110] we may tabulate the probability W that an electron of initial energy E_0 in passing through a "thickness" $b\ell$ has energy E greater than fE_0.

Table V

Straggling of electron energies in tantalum. W is the probability that an electron of initial energy E_0 has final energy greater than $f\,E_0$ after passing through a foil

Thickness of Ta (g/cm^2)	$b\ell$	W		
		f = 0.98	f = 0.95	f = 0.90
0.049	0.01	0.967	0.976	0.982
0.097	0.02	0.935	0.952	0.965
0.146	0.03	0.904	0.928	0.948
0.194	0.04	0.874	0.906	0.930
0.243	0.05	0.845	0.883	0.913

Figure 7 shows the distribution of electron energies resulting from the passage of a beam of electrons of energy E_0 through the thickest converter used when only radiation loss is considered. In the spectrometer the electrons are being produced uniformly throughout the thickness of the converter, so that, for a particular E_0, the resulting distribution is sharper. To evaluate the effect of straggling on the measured photon spectrum it is necessary to consider the fact that the energy of the photon is divided between the electron and positron. Aamodt[111] has shown that for a converter as thin as 0.02 in. of Ta ($\sim$7 times our thickness) the effective straggling in the measured photon spectrum, after these processes are taken into account, is the same as the straggling experienced by an electron of energy E_γ passing through the full thickness of the converter. Hence, for a 15.1-Mev photon, 90% of the counts would be contained in an energy width of less than 0.01 x 15.1 = 0.15 Mev. This represents an insignificant effect with respect to the other factors influencing the resolution of the spectrometer and hence has been neglected.

4. Pair-Spectrometer Efficiency

The efficiency of a magnetic pair spectrometer is limited by the scattering of the electrons in the converter foil. The magnitude of this effect is of most importance for lower-energy gamma rays, since scattering is greatest for low-energy electrons. Therefore, there are two factors working to reduce the efficiency of the pair spectrometer for low-energy gamma rays: (a) the pair-production cross section is smaller for low energies, and (b) the converter thickness must be reduced to keep the scattering corrections reasonable. During the course of the experiments discussed in this thesis it was necessary to use the spectrometer to measure the relative intensities of gamma rays of $\sim$ 10 to 15 Mev energy. The method of calculating the efficiency of the pair spectrometer when a continuous spectrum is being analyzed is presented in Reference 1. However, since it was desired that the line shape of the spectrometer for gamma rays of various energies be known, as well as the efficiency, a more complicated calculational program was attempted using the IBM 650 Computer.

The geometry of the apparatus is shown diagrammatically in Fig. 23, in which the converter and the effective area of the counters are in the XY plane, and the magnetic field is directed along the X axis, and the γ-ray beam is parallel to the Z axis. In the pair spectrometer the X axis is the vertical axis and the Y axis is the horizontal axis. Neglecting the small displacement arising from scattering in the converter, we can consider the electron-positron pair to leave the converter at the point (x, y). Let the momentum vectors p^+, p^- for the positron and the electron have polar angles θ^+, θ^-. Let the angles between the projection of the momentum vectors in the XZ plane and the Z axis be θ+v and θ-v, and similarly, for the YZ plane, let the angles be θ + H and θ = H. After being deflected by the magnetic field, the electron and positron enter the XY plane at the coordinates (x-, y-) and (x+, y+), respectively.

The probability that an electron of proper energy will enter the sensitive area defined by the coordinates Y_1 and Y_2 is determined by θ_V and, similarly, θ_H determines the probability that the electron of proper energy will enter the area defined by the coordinates X_1 and X_2.

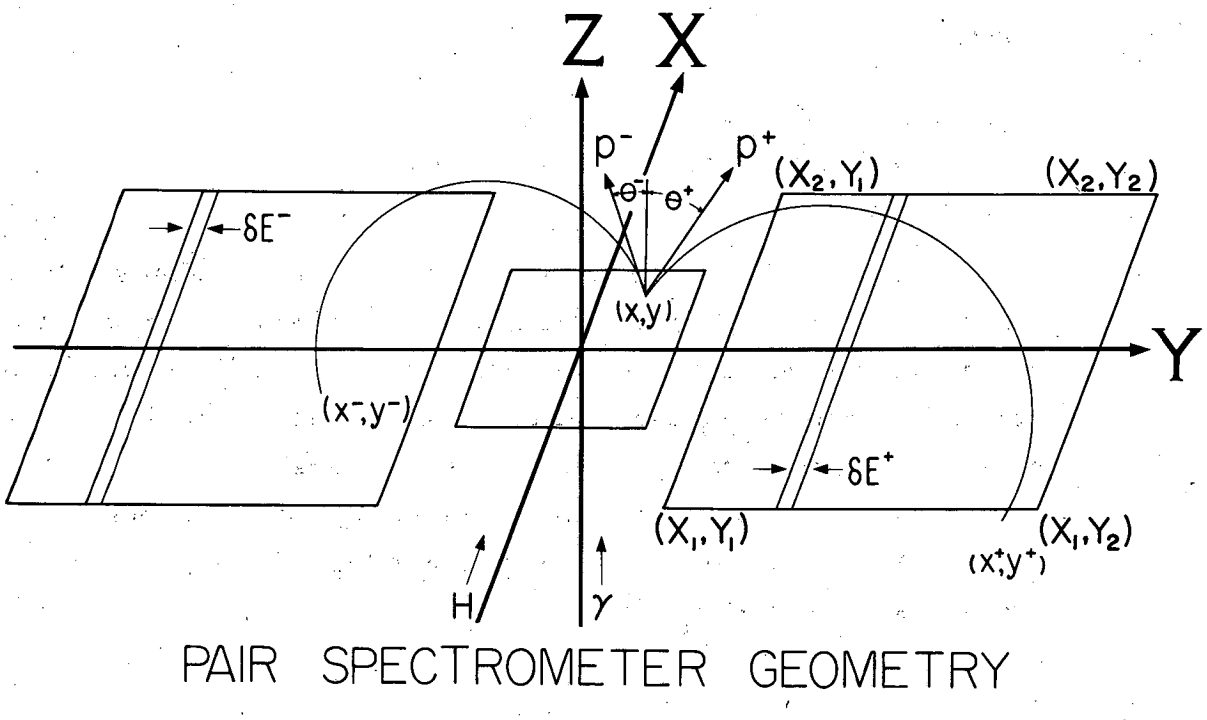

Fig. 23. Geometry of the pair spectrometer.

Since the apparent energy of the γ ray is determined by $y+ + y-$, the line shape of the spectrometer is determined by θ_H. It is shown in Appendix II that the angular distributions in θ_V and θ_H are the same and that, to a very good approximation, they are Gaussian with a root-mean-square angle:

$$\theta_{rms} = \frac{1}{\sqrt{2}} \theta_C = \frac{1}{\sqrt{2}} \frac{21}{T} \frac{Z^{1/2}}{X_0} ,$$

where

T = kinetic energy in Mev,

Z = thickness of scattering material,

X_0 = radiation length.

Thus it is possible to divide the efficiency and line-shape calculations into two steps: first, the evaluation of the effect of horizontal scattering, assuming infinite extent of the counters in the X direction, and secondly, multiplying these efficiencies by the probability that the pairs enter within the vertical extent of the counters.

The 180° geometry of the spectrometer gives us the relationship that the apparent energy of an electron of energy E_0 emitted at an angle θ_H is

$$E = E_0 \cos \theta_H .$$

Thus, if the distribution is Gaussian, the probability that an electron has an apparent energy between Ej and Ej_{-1} is

$$P_{j, j-1} = \frac{2}{\sqrt{\pi}} \int_{t_{j-1}}^{t_j} e^{-t^2} \, dt ,$$

where

$$t_j = \frac{\theta_j}{\theta_C} = \frac{\cos^{-1} \frac{E_j}{E_0}}{\frac{21}{T} \frac{Z^{1/2}}{X_0}} ,$$

and E_0 is determined by E_γ, the energy of the gamma ray, and the parameter v, where v is the energy of the positron divided by the energy of the gamma ray. The value of Ej is determined by the value of the magnetic field and the coordinates y and $y_\pm$. By letting $Ej - Ej_{-1} = 0.15$ Mev, we may calculate the probability that, for a particular v-splitting, the electron and positron will be in a particular energy channel 0.15 Mev wide. Weighting each v-splitting by the probability that such a splitting is produced, and summing over all v's, we obtain the line shape. This calculation was performed for five strips along the Y axis and five thicknesses of converter material. For each of these combinations the line shape was calculated for 10.7- and 15.1-Mev gamma rays for both magnetic field settings used in the experiments.

The correction for vertical scattering does not involve the focusing properties of the magnetic field, therefore the fraction of the electrons intercepted by the sensitive area is given by

$$E_v = \frac{1}{\sqrt{\pi}} \int_{t_1}^{t_2} e^{-t^2} \, dt ,$$

where, from Fig. 23, we have

$$t_1 = \frac{\theta_1}{\theta_C} = \frac{\tan^{-1} \dfrac{X_1 + x}{\pi(y_\pm - y)}}{\dfrac{21}{T} \dfrac{Z^{1/2}}{X_0}}$$

and

$$t_2 = \frac{\theta_2}{\theta_C} = \frac{\tan^{-1} \dfrac{X_2 - x}{\pi(y_\pm - y)}}{\dfrac{21}{T} \dfrac{Z^{1/2}}{X_0}} .$$

For the angles θ_1 and θ_2 involved in the spectrometer we may approximate

$$\tan \theta \simeq \theta ,$$

with the result

$$t_{1,2} = \frac{\dfrac{X_{1,2} \pm x}{\pi(y_{\pm} - y)}}{\dfrac{21}{T}\,\dfrac{Z^{1/2}}{X_0}} .$$

Since we are dealing with relativistic electrons,

$$y_{\pm} - y = a(H)\, T ,$$

where $a(H)$ is a parameter dependent only on the field.

Therefore we have

$$t_{1,2} = \frac{X_{1,2} \pm x}{\pi\, a(H)} \Big/ \frac{21\, Z^{1/2}}{X_0} .$$

and the vertical scattering correction is the same for all gamma rays measured with a fixed magnetic field.

The vertical scattering correction was calculated for six converter strips taken along the X axis. In the horizontal-scattering calculation the line shape changed considerably from one thickness to the other but the efficiency remained practically constant. However, the vertical scattering affects the efficiency directly, therefore the converter was divided into nine thicknesses, four of which were within the first thickness used for the horizontal scattering calculation.

In summary, the efficiency of the spectrometer is determined primarily by the vertical scattering, and the line shape is determined by the horizontal scattering. Horizontal scattering does have a slight effect on the efficiencies of the end channels, slightly increasing the efficiency of the higher-energy channels and slightly decreasing the efficiency of the lower-energy channels. The correction for vertical scattering is the same to first order for all gamma rays measured at a fixed magnetic field.

An additional uncertainty exists when the losses due to vertical scattering are significant, since some of the scattered electrons can reflect from the pole tips and be counted. The pole tips were lined

with Al to reduce the magnitude of this effect. An empirical test of the efficiency calculations was made by comparing the counting rates for 15.1-Mev gamma rays obtained with two field settings with a thin converter (0.0294 g/cm^2 Ta). The calculated ratio is 3.76, and that observed is 3.86 ± 0.23.

A further test of the efficiency calculations was made by comparing the counting rates obtained with two different converters (0.0294 and 0.1397 g/cm^2 Ta) at a fixed magnetic field. Here, the calculated ratio is 1:99 and the observed ratio is 3.22 ± 0.23.

The thin-converter calculation gives excellent agreement with measurement, but the thick-converter yield is higher than the computed yield. The correction for vertical scattering is large for the thick converter and thus indicates that electrons might be expected to scatter from the pole tips. This is confirmed by the fact that the calculated line shape agrees quite well with the observed shape for the thin converter, but that the thick-converter line shape was broader than the calculated line shape. Only data obtained with the thin converter were used to determine cross sections, and the thick converter was used to obtain the excitation function, since its efficiency was three times that of the thin converter.

REFERENCES

1. D. Cohen, Bremmstrahlung from Proton Bombardment of Nuclei (Thesis), UCRL-3230, Dec. 1955.
2. D. Cohen, B. J. Moyer, H. Shaw, and C. N. Waddell, - To be published.
3. Cohen, Moyer, Shaw, and Waddell, Phys. Rev. 96, 714 (1954).
4. F. Ajzenberg and T. Lauritsen, Revs. Modern Phys. 27, 77 (1955).
5. V. R. Johnson, Phys. Rev. 86, 302 (1952).
6. T. W. Bonner and J. E. Evans, Phys. Rev. 73, 666 (1948).
7. P. Morrison, in Experimental Nuclear Physics, E. Segrè, Ed., New York, 1953, Vol. II, pp. 89-95.
8. Cohen, Moyer, Shaw, and Waddell, Phys. Rev. 95, 664 (1954).
9. Rasmussen, Rees, Sampson, and Wall, Phys. Rev. 96, 812L (1954).
10. R. K. Adair, Phys. Rev. 87, 1041 (1952).
11. N. M. Kroll and L. L. Foldy, Phys. Rev. 88, 1177 (1952).
12. F. Ajzenberg and T. Lauritsen, Isobars: A = 5 to 20, in Quarterly Report No. 4 - Appendix B, Dept. of Physics, Boston University, September, 1954.
13. C. A. Barnes and R. W. Kavanagh, Phys. Rev. 100, 1996A (1955).
14. R. W. Kavanagh, Scintillation and Magnetic Spectrometer Studies of Nuclear Reactions (Ph. D. Dissertation), California Institute of Technology, 1956.
15. Marion, Bonner, and Cook, Phys. Rev. 100, 847 (1955).
16. Bigham, Allen, and Almqvist, Phys. Rev. 99, 631A (1955).
17. Gove, Litherland, Almqvist, Bromley, and Fergusen, Bull. Am. Phys. Soc. II, 2, 51 (1957).
18. H. E. Gove, (Chalk River Lab.) private communication.
19. Fuller, Hayward, and Svantesson, Bull. Am. Phys. Soc. II, 6, 197 (1956).
20. E. Hayward and E. G. Fuller, Physica 22, 1138 (1956).
21. E. G. Fuller and E. Hayward, Phys. Rev. 106, 991 (1957).

22. J.E. Leiss and J.M. Wyckoff, Bull. Am. Phys. Soc. II, 1, 197 (1956).
23. K.H. Spring, Photons and Electrons (Methuen, London, 1950).
24. R.L. Walker and B.D. McDaniel, Phys. Rev. 74, 315 (1948).
25. B.B. Kinsey and G.A. Bartholomew, Can. J. Phys. 31, 315 (1948).
26. R. Hofstadter, Phys. Rev. 74, 100 (1948).
27. J. Birks, Scintillation Counters (Pergamon, London, 1953).
28. S.C. Curran, Luminescence and the Scintillation Counter (Buttersworths, London, 1953).
29. S.C. Curran, Advances in Physics, Phil. Mag. Quarterly Suppl. 2, 411 (1953).
30. W.M. Jordon, Detection of Nuclear Particles in Ann. Rev. Nuclear Sci. 1, Stanford, (1952).
31. P.R. Bell, in Beta- and Gamma-Ray Spectroscopy, K. Siegbahn Ed., Interscience New York, 1955).
32. G.R. White, "X-ray Attenuation Coefficients from 10 kev to 100 Mev." Natl. Bur. Standards (U.S.) Report No. 1003, 1952.
33. C.M. Davisson, in Beta- and Gamma-Ray Spectroscopy, K. Siegbahn, Ed. (Interscience, New York, 1955).
34. J.G. Campbell and A.J.F. Boyle, Australian J. Phys. 6, 171 (1953).
35. J.G. Campbell and A.J.F. Boyle, Australian J. Phys. 7, 284 (1954).
36. G.M. Griffiths, Can. J. Phys. 33, 209 (1954).
37. R.S. Foote and H.W. Koch, Rev. Sci. Instr. 25, 746 (1954).
38. H.R. Bowman and R.E. Thomas, Multichannel Pulse-Height Analyzer UCRL-2164, April 1953.
39. Bjorklund, Crandall, Moyer, and York, Phys. Rev. 77, 213 (1950).
40. W. Crandall and B.J. Moyer, Phys. Rev. 92, 749 (1953).
41. Shaw, Cohen, Moyer, and Waddell, Bull. Am. Phys. Soc. I, 29, 11 (1954).
42. R. Serber, Phys. Rev. 72, 1114 (1947).
43. W.N. Hess, A Summary of High-Energy Nucleon-Nucleon Cross-Section Data, UCRL-4639, May 1956.
44. D.C. Peaslee, Nuclear Reactions of Intermediate Heavy Particles, in Ann. Rev. of Nuclear Sci. V (1955).

45. M.L. Goldberger, Phys. Rev. 74, 1269 (1948).
46. Morrison, Muirhead, and Rossen, Phil. Mag. 44, 1326 (1953).
47. Fernbach, Serber, and Taylor, Phys. Rev. 75, 1352 (1949).
48. Hayakawa, Kawai, and Kikuchi, Progr. Theoret. Phys. (Kyoto) 13, 415 (1955)
49. L.R.B. Elton and L.C. Gomes, Phys. Rev. 105, 1027 (1957).
50. R.M. Eisberg and G. Igo, Phys. Rev. 93, 1039 (1954).
51. George J. Hecht, Angular Distributions of Charged Particles from 31-Mev Protons on Carbon (Thesis), UCRL-2969, April 1955.
52. R.G. Finke, Charged Particles from Beryllium Bombarded by 31.3-Mev Protons (Thesis), UCRL-2789 Nov. 1954; Beneveniste, Finke, and Martinelli, Phys. Rev. 101, 655 (1956).
53. Austern, Butler, and McManus, Phys. Rev. 92, 350 (1953).
54. K. Strauch and F. Titus, Phys. Rev. 103, 200 (1956).
55. B. Rossi, High-Energy Particles, (Prentice-Hall, New York, 1952) Sect. 2.16.
56. Blatt and Weisskopf, Theoretical Nuclear Physics, (Wiley, New York, 1952) Chapters VII-X.
57. P. Morrison, in Experimental Nuclear Physics, E. Segrè, Ed., Vol. II, (Wiley, New York, 1953).
58. Helmholz, McMillan, and Sewell, Phys. Rev. 72, 1003 (1947).
59. R. Serber, Phys. Rev. 72, 1008 (1947).
60. C. Wiegand, Rev. Sci. Instr. 19, 790 (1948).
61. R.K. Adair, Phys. Rev. 87, 1041 (1952).
62. N.M. Kroll and L.L. Foldy, Phys. Rev. 88, 1177 (1952).
63. Cook, Fowler, Lauritsen, and Lauritsen, to be published.
64. S.A. Moszkowski in Beta- and Gamma-Ray Spectroscopy, K. Siegbahn, Ed., (Interscience, New York, 1955).
65. E.G. Fuller and E. Hayward, private communication.
66. I.C. Biedenharn and M.E. Rose, Revs. Modern Phys. 25, 729 (1953).
67. Sharp, Kennedy, Sears and Hoyle; Tables of Coefficients for Angular Distribution Analysis, Chalk River Project Report CRT-556, Dec. 1953.

68. E. Almqvist, private communication.
69. M. G. Mayer, Phys. Rev. 78, 16 (1950).
70. M. G. Mayer and J. H. D. Jensen, Elementary Theory of Nuclear Shell Structure, (Wiley, New York, 1955).
71. S. A. Moszkowski, Phys. Rev. 89, 474 (1953).
72. M. E. Rose, Multipole Fields (Wiley, New York, 1955).
73. D. H. Wilkinson, Phil. Mag. VIII, 1, 127 (1956).
74. E. P. Wigner, Phys. Rev. 51, 106 (1937).
75. B. Cassen and E. U. Condon, Phys. Rev. 50, 846 (1936).
76. Blatt and Weisskopf, Theoretical Nuclear Physics, (Wiley, New York, 1952) Chapter VI.
77. L. E. Trainor, Phys. Rev. 85, 962 (1952).
78. L. A. Radicati, Phys. Rev. 87, 521 (1952).
79. M. Gell-Mann and V. L. Telegdi, Phys. Rev. 91, 169 (1953).
80. W. MacDonald, Phys. Rev. 98, 60 (1955).
81. F. C. Barker and A. K. Mann, Phil. Mag. VIII, 2, 5 (1957).
82. D. H. Wilkinson and G. A. Jones, Phil. Mag. VII, 44, 1269 (1953).
83. D. H. Wilkinson, Phil. Mag. VII, 44, 1019 (1953).
84. A. B. Clegg, and D. H. Wilkinson, Phil Mag. VII, 44, 1269 (1953).
85. D. H. Wilkinson and A. B. Clegg, Phil Mag. VII, 44, 1322, (1953).
86. G. A. Jones, and D. H. Wilkinson, Phil Mag. VII, 45, 703, (1954).
87. D. H. Wilkinson and A. B. Clegg, Phil. Mag. VIII, 1, 291 (1956).
88. D. H. Wilkinson, Phil. Mag. VIII, 1, 379 (1956).
89. Bloom, Toppel, and Wilkinson, Phil. Mag. VIII, 2, 57 (1957).
90. D. H. Wilkinson and S. D. Bloom, Phil. Mag. VIII, 2, 63 (1957).
91. L. A. Radicati, Proc. Phys. Soc. A, 66, 139 (1953).
92. R. MacDonald, Phys. Rev. 101, 271 (1956).
93. Blatt and Weisskopf, Theoretical Nuclear Physics (Wiley, New York, 1952), Chapter X.
94. R. W. Hill, Phys. Rev. 90, 845, (1953).
95. J. R. Cameron, Phys. Rev. 90, 839 (1953).
96. Rasmussen, Miller, and Sampson, Phys. Rev. 100, 181 (1955).
97. T. Teichmann and E. P. Wigner, Phys. Rev. 87, 123 (1952).
98. E. U. Baranger, Phys. Rev. 99, 145 (1955).

99. F.C. Barker, Phil. Mag. VIII, 2, 286L (1957).

100. F. J. Vaughn, Elastic and Inelastic Scattering of 48-Mev Alpha Particles by Carbon and Magnesium (Thesis), UCRL-3174, Oct. 1955.

101. H. Bethe and W. Heitler, Proc. Roy. Soc. A (London) 146, 83, (1934).

102. W. Heitler, Quantum Theory of Radiation, 3d Ed., (Clarendon, Oxford, 1954), Sect. 25.

103. L. Simons and K. Zuber, Proc. Roy. Soc. A (London) 159, 383 (1937).

104. L. V. Groshev and I. M. Frank, Compt. rend. acad. sci. (U.R.S.S.) 20, 273 (1938), and 24, 239 (1941).

105. L. V. Groshev, J. Phys. (USSR) 5, 115 (1941).

106. H. Bethe and J. Ashkin, in Experimental Nuclear Physics, E. Segrè, Ed., Vol. 1 (Wiley New York, 1953).

107. W. Paul and H. Steinwedel, in Beta- and Gamma-Ray Spectroscopy, K. Siegbahn, Ed., (Interscience New York, 1955).

108. J. A. Richards and, L. W. Nordheim, Phys. Rev. 74, 1107 (1948).

109. L. Eyges, Phys. Rev. 76, 264 (1949); Phys. Rev. 77, 81 (1950).

110. K. Pearson, in Tables of the Incomplete Γ-Function, K. Pearson, Ed. (Biometrika, London, 1922).

111. R. L. Aamodt, Gamma-Ray Spectrum from the Absorption of Negative Pi Mesons in Deuterium (Thesis), UCRL-1151, March 1951.